Water Research 186 (2020) 116140

Contents lists available at ScienceDirect

Water Research

journal homepage: www.elsevier.com/locate/watres

Particle association of *Enterococcus* sp. increases growth rates and simulated persistence in water columns of varying light attenuation and turbulent diffusivity

Elise M. Myers [a, b, *], Andrew R. Juhl [a, b]

[a] Columbia University, 535 W 116th Street, New York, NY, 10027, USA
[b] Lamont Doherty Earth Observatory, 61 Route 9W, Palisades, NY, 10964, USA

ARTICLE INFO

Article history:
Received 12 March 2020
Received in revised form
22 June 2020
Accepted 2 July 2020
Available online 17 August 2020

Keywords:
Sewage
Wastewater
Fecal indicator bacteria
Inactivation
Water quality
T90

ABSTRACT

Predicting water quality and the human health risks associated with sewage-derived microbes requires understanding the fate and transport of these contaminants. Sewage-derived pathogen risks are typically assessed and monitored by measuring concentrations of fecal indicating bacteria (FIB), like *Enterococcus* sp. Previous research demonstrated that a high fraction of FIB is particle-associated, which can alter FIB dynamics within secondary water bodies. In this study, we experimentally quantified the effect of particle association on dark, temperature- and light-dependent growth and sinking rates of enterococci. Particle association significantly increased dark growth rates, light-dependent growth rates (i.e. decreased mortality), and sinking rates, relative to free-living enterococci. Simulations using a novel, 1-dimensional model parameterized by these rates indicate greater persistence (T_{90}) for particle-associated enterococci in water bodies across a wide range of diffuse attenuation coefficients of light (K_d) and turbulent diffusivity (D) values. In addition, persistence of both fractions increased in simulated turbid and turbulent waters, compared to clear and/or quiescent conditions. Simulated persistence of both fractions also increased when enterococci discharges occurred later in a diel cycle (towards sunset, as opposed to sunrise), especially for the free-living population, because later discharges under our model conditions allowed both fractions to mix deeper before inactivation via sunlight. Model sensitivity testing revealed that T_{90} variability was greatest when dark growth rates were altered, suggesting that future empirical studies should focus on quantifying these rates for free-living and particle-associated sewage-derived microbes. Despite greater sensitivity of T_{90} to variability in dark growth rates, omitting light-dependent growth rates from simulations dramatically influenced T_{90} values. Our results demonstrate that particle association can increase enterococci persistence in receiving waters and highlight the importance of incorporating particle association in future water quality models.

1. Introduction

Sewage pollution of coastal environments is a common management concern due to the public health risks from contact with water contaminated with pathogenic bacteria, protozoa, and viruses (Horman et al., 2004; Fong and Lipp, 2005). With increasing urbanization, particularly in coastal regions, there is increased potential for degradation of surface waters by sewage discharges (Vermeulen et al., 2015). Management of health risks related to sewage pollution relies on in-field monitoring programs and statistical or numerical modeling to predict water quality or untreated discharges.

Fecal indicator bacteria (FIB) include several types of bacteria used to indicate contamination by sewage and co-occurring pathogens. FIB are generally assumed to have limited environmental persistence, so have long been interpreted as indicating recent fecal pollution (Litsky et al., 1953). However, prolonged persistence reported under some conditions (Bordalo et al., 2002; Anderson et al., 2005; Chudoba et al., 2013) complicates FIB use as sewage pollution indicators. Commonly used FIB include total coliforms, fecal coliforms, *Escherichia coli*, and *Enterococcus* sp., though only *Enterococcus* sp. is approved by the US Environmental Protection Agency (EPA) for testing water quality in brackish to salty water bodies (US EPA, 2012). Enterococci abundance in recreational waters correlates

* Corresponding author. Columbia University, 535 W 116th Street, New York, NY, 10027, USA.
E-mail address: emyers@ldeo.columbia.edu (E.M. Myers).

https://doi.org/10.1016/j.watres.2020.116140

with increasing incidence of gastrointestinal illness in swimmers, particularly when the source is sewage or other wastewater (Cabelli et al., 1982; Wade et al., 2003; Colford et al., 2012).

Effectively predicting concentrations of FIB and co-occurring pathogens in surface waters requires considering their ecological dynamics when they transition from the gastrointestinal tract to secondary habitats (Gordon et al., 2002), like storm water, wastewater, and receiving waters. The "extra-enteric ecology" (Boehm et al., 2005; O'Mullan et al., 2017) of FIB is dominated by loss processes, including inactivation (Evison, 1988; Howell et al., 1996), predation (McCambridge and McMeekin, 1981; Menon et al., 2003), transport (Cho et al., 2010), and dispersion (Nevers and Boehm, 2011). While physical advection and diffusion are critical for understanding FIB distributions, models that omit FIB inactivation typically perform poorly relative to observations, even over very short time and space scales (e.g. over a few hours and only 100s of meters, Rippy et al., 2013a,b). Such results suggest that FIB inactivation or growth can be at least as important for predicting FIB distributions as hydrodynamics. In many FIB models, bacteria are transported with the water, while the population decays according to a constant rate (Bedri et al., 2011; Banas et al., 2015; Wen et al., 2017), or a decay rate that varies with temperature (e.g., Chen and Liu, 2017) and/or light exposure (Cho et al., 2010) along the flow path. However, if FIB movement diverges from that of the water, or if inactivation rates are incorrectly parameterized, then numerical simulations will deviate from actual conditions, even if the model accurately represents complex hydrodynamics.

Light exposure causes inactivation of FIB and associated pathogens (Evison, 1988; Sinton et al., 2002; Kay et al., 2005), making photoinactivation rates critical to FIB models. Light-induced FIB inactivation rates can be modified by suspended solids or turbidity (Whitman et al., 2004; Kay et al., 2005; Gutiérrez-Cacciabue et al., 2016), water column depth, and time of day (Davies-Colley et al., 1994; Sinton et al., 2002). Sunlight can cause inactivation through two pathways: 1) direct solar radiation damage to nucleic acids and other cellular components (Malloy et al., 1997; Schuch and Menck, 2010) and/or 2) the photochemical generation of reactive oxygen species from organic matter (Maraccini et al., 2012; Appiani and McNeill, 2015). Both mechanisms are likely important for enterococci as both UV radiation and visible light cause enterococci decay (i.e. negative light-dependent growth; Davies-Colley et al., 1994; Fujioka and Yoneyama, 2002; Sinton et al., 2002).

Also critical to extra-enteric ecology are FIB growth rates in the absence of light exposure (i.e. dark growth rates), which encompass a wide variety of processes, such as cell division rates, predation, and stress-induced losses. Generally, increasing temperatures are linked to higher FIB inactivation (Auer and Niehaus, 1993; Schulz and Childers, 2011; Boehm et al., 2018) while lower temperatures tend to increase FIB persistence (Bordalo et al., 2002; Lleodel et al., 2005). Increased nutrients (e.g. phosphate) have been shown to enhance FIB persistence and growth in the dark (Chudoba et al., 2013). Meanwhile, elevated salinity has been reported to increase (Okabe and Shimazu, 2007; Schulz and Childers, 2011), decrease (Bordalo et al., 2002; Anderson et al., 2005), or minimally impact (Noble et al., 2004; Ahmed et al., 2014; Chen and Liu, 2017) growth rates of various FIB. Net growth rate measurements in ambient waters in darkness thus encompass the effects of multiple abiotic and biotic properties impacting FIB persistence.

High frequency of FIB particle association (Fries et al., 2006; Krometis et al., 2007; Cizek et al., 2008; Walters et al., 2014), often greater than that of the background bacterial community (Ducklow et al., 1982; Suter et al., 2011), further complicates these dynamics. Particle association is thought to prolong FIB environmental persistence (O'Mullan et al., 2017) because particles may provide a more favorable environment than the surrounding water (Lyons et al., 2007, 2010), due to increased nutrient or solute availability (Shanks and Reeder, 1993; Kiørboe and Jackson, 2001), physical stability (Craig et al., 2002), and protection from predation (Davies and Bavor, 2000) or other stressors like chemical disinfectants (Hess-Erga et al., 2008). However, bacterivory can also increase on particles (Lee et al., 2011), potentially mitigating some advantages. Actual growth rate measurements separating particle-associated and free-living FIB are rare. Garcia-Armisen and Servais (2009) found particle-associated *E. coli* dark decay rates in river water to be about 2.5 times lower than rates for free-living cells. Similar rates for enterococci or other FIB have not previously been reported.

Particle-associated FIB are also likely to have appreciable sinking rates (Auer and Niehaus, 1993; Garcia-Armisen and Servais, 2009). Although many FIB are associated with smaller particles (Auer and Niehaus, 1993; Jamieson et al., 2004; Ahn et al., 2005; Mote et al., 2012), implying relatively slow sinking, any sinking could impact horizontal transport and eventually lead to deposition in sediments, especially in shallow water. It is now well-established that sediments can constitute a reservoir of settled FIB that can be resuspended (Jamieson et al., 2005a; Fries et al., 2008; O'Mullan et al., 2019), highlighting the importance of FIB particle association.

Unfortunately; the empirical observations needed to separately parameterize particle-associated and free-living FIB populations within water quality models are very limited to date. Some models used for stream water quality assessment incorporate FIB particle association using a free-living FIB population transported with the water and a second FIB population transported with sediment (Jamieson et al., 2005b; Yang et al., 2008; Wu et al., 2009; Kim et al., 2010). However, as pointed out in Cho et al. (2016), while different growth rates for these two FIB populations could readily be included in such models, "investigations are not yet robust enough to effectively determine rate constants for both bacteria populations." Two recent estuarine FIB distribution models (de Brauwere et al. 2014; Chen and Liu, 2017) included explicit representation of particle-associated and free-living populations; however, neither model included light inactivation. Both studies acknowledged the potential importance of light-dependent rates, but also cited a lack of information for appropriate parameterization. We are aware of only one previous study investigating light inactivation in combination with particle association. Using artificial sunlight (Walters et al., 2014), found greater light-induced inactivation of FIB that were free-living or associated with small particles (<12 μm) in sewage effluent, compared to those on larger particles (12−63 μm). With the exception of the aforementioned *E. coli* study (Garcia-Armisen and Servais, 2009), separate dark growth rates for particle-associated and free-living FIB have also not been previously measured. In addition, while a few empirical FIB sinking rate measurements are available (Auer and Niehaus, 1993; Garcia-Armisen and Servais, 2009), enterococci sinking rates have not yet been reported.

In this study, we address the hypothesis that particle association increases the persistence of enterococci by providing a more favorable environment. Our study combines empirical quantification of growth and sinking rates with a 1-dimensional model simulating persistence according to those rates under conditions representing different types of water bodies. This is the first work we are aware of that separately quantifies the rates of light-dependent growth, dark, temperature-dependent growth, and sinking for both free-living and particle-associated fractions of enterococci. Further, we use these rates in simulations to examine how water column persistence of each enterococci fraction could change in water bodies with different levels of turbidity and turbulence. Model sensitivity to growth and sinking rate parameterization was tested through additional simulations. Finally, we use

simulations to examine the potential impact of discharge timing within a diel cycle on overall enterococci persistence.

2. Methods

2.1. Empirical rate determination

2.1.1. Study site

Near-surface water samples were collected from two sites along the Piermont Pier (Piermont, NY, USA) that are subject to intermittent municipal sewage pollution, 1) near the Orangetown and Rockland County Sewer District Wastewater Treatment Plant Outfalls and 2) near a sewage pump station that occasionally overflows, and a third nearby site along the frequently sewage-contaminated tributary, Sparkill Creek (Fig. A1, O'Mullan et al., 2019 provides additional information about these sites). Salinity near Piermont Pier ranged from 0.2 to 10 ppt, consistent with its location in the brackish, tidal portion of the Hudson River Estuary (HRE). At each sample collection, either a Hydrolab HQ 40D meter (light and temperature growth rate experiments) or Hydrolab DS5 (sinking rate experiments) was used to measure temperature, salinity, and dissolved oxygen (HQ 40D) or turbidity (DS5). Water clarity was measured using a 300-mm diameter Secchi disk. See Tables A1 and A4 for environmental data for experiments.

2.1.2. Microbial culturing

Near-surface water samples were collected via bucket cast and stored in sterile polypropylene bottles that were triple rinsed with sample water directly prior to collection. Samples were immediately transferred to dark coolers until laboratory processing, within 2 h of sample collection. The particle-associated and free-living bacterial fractions were separated following Crump et al. (1999) and Suter et al. (2011). Water samples were filtered under gentle vacuum pressure through 47-mm diameter, 3-μm pore polycarbonate membrane filters. Filtration was paused when a thin film of liquid remained above the filter. The filtrate, containing the free-living fraction, was collected. Then, the particle-associated fraction (above the filter) was diluted with sterile Phosphate Buffered Saline (PBS, 0.1 M phosphate in 0.73% NaCl) and gently filtered again until a thin film of liquid once again remained above the filter. The separation step resulted in small losses from both fractions; in tests ($n = 8$), a mean of 12.8% of the total count passed through the filter on the second filtration step. This minor loss from both fractions did not affect our experiments, which only required consistently separating the two subpopulations from each other. The particle-associated fraction was rinsed from the filter tower three times with PBS and this supernatant was transferred into sterile 250-mL polypropylene bottles on a shaker table (80 rpm for 6 min) to detach microbes from particles. The particle-associated fraction was reconstituted to the original volume with PBS. No viable cells remained on the rinsed polycarbonate membrane filters (processed following EPA Method 1600 for enterococci enumeration (US EPA, 2002), $n = 6$).

For each fraction, 1–3 subsamples (ranging 1–100 mL) were filtered onto 0.45-μm gridded, mixed-ester cellulose membrane filters. These filters were incubated on sterile, solid mEI media for 24 h at 41 °C following EPA Method 1600. Colony forming units (CFUs) on each plate were normalized to CFU/100 mL in the original sample. Total enterococci counts (the sum of both fractions) were also calculated for each water sample for comparison with previous work.

2.1.3. Quantifying dark, temperature-dependent growth rates

Because FIB concentrations typically decline over time in experiments, other studies use terminology such as "inactivation", "mortality", "die-off", or "decay" rates to describe the dynamics. In our experiments, counts occasionally increased over time, so we use the term "growth rate" in this study; negative growth rates imply a decline in enterococci concentration over time.

To quantify dark, temperature-dependent growth rates, a water sample was mixed and divided into 3 sterile, 250-mL polypropylene bottles, that were then placed into 3 dark incubators set to 5, 18, and 28 °C, respectively. Aliquots (125 mL) were removed from gently homogenized bottles after 24 and 48 h. The free-living and particle-associated enterococci remaining in each aliquot were separated and enumerated as described above. For every timepoint of each experiment, multiple subsamples of different volumes were filtered to ensure some plates would be countable. Values used in rate calculations were then averaged from 2 to 3 plates per timepoint.

2.1.4. Quantifying light-dependent growth rates

For each experiment, a water sample was mixed and subsamples (approximately 250 mL) were added to sterile, UV-permeable Whirlpak sampling bags, that were then placed into an outdoor, 18 °C water bath exposed to full sun. This temperature was chosen for experiments because enterococci dark, temperature-dependent growth rates at 18 °C are relatively low (Table 1). Experiments were started near mid-day on days with minimal cloud cover. Downwelling photosynthetically active radiation (PAR) was measured using a Li-COR Quantum cosine-corrected sensor recording to a LI-1400 Data Logger for normalization between experiments (Table A3). Subsamples collected from the bags after 1 and 2 h of sunlight exposure were processed to separate and enumerate free-living and particle-associated enterococci as described above. Also as described above, for every timepoint of each experiment, multiple subsamples of different volumes were filtered. When multiple plates were countable, the values were averaged.

2.1.5. Growth rate calculation

For both temperature- and light-dependent growth rate experiments, the concentrations of particle-associated and free-living enterococci in each container were natural log (ln) transformed and plotted against time. The slope of the linear best fit to the ln-transformed data provided the first-order exponential growth rate (day^{-1}), as in other studies (Sinton et al., 2002; Anderson et al., 2005; Maraccini et al., 2016).

2.1.6. Statistical analysis of growth rates

Statistical analysis was conducted using R statistical software. Normal distribution of empirically-determined growth rates within each treatment was confirmed via a Shapiro-Wilk test ($p > 0.1$). Two-way analysis of variance (ANOVA) tests with $\alpha = 0.05$ were used to compare mean growth rates for temperature-dependent experiments followed by Fisher's Least Significant Difference (LSD) *post hoc* pairwise comparisons. An unequal variances *t*-test without pairing (due to unequal sample numbers), was used to test the impact of light on mean growth rates of the two fractions.

2.1.7. Quantifying sinking rate distributions

Approximately 25 L of surface water was collected from the end of Piermont Pier (Fig. A1), on 5 dates (Table A4). Experiments began within 2 h of collection in a temperature-controlled room set to match the original sample temperature (±2 °C). Following Aumack and Juhl (2015), we used a homogenous suspension (Bienfang et al., 1977; Chancelier et al., 1998) approach to measure the sinking rates of inorganic particles, organic particles, particle-associated, and free-living enterococci. A series of replicate 0.4 m high, (2.3 L total volume) graduated cylinders were used as settling columns, with one column per time point. At each time point, the upper 2-L portion of a given settling column was carefully pumped off,

Table 1
Parameter Definition and Values. Empirically-determined and literature-based values used in the model are shown alongside parameter definitions.

Parameter	Variable	Units	Values	Definition
Dark, Temperature-Dependent Growth	λ_{Temp}	day^{-1}	FL: -0.359 PA: 0.33	Growth rate of enterococci cells under different temperatures (negative is mortality)
Light-Dependent Growth	λ_{Light}	day^{-1}	FL: -33.31 PA: -16.48	Growth rate of enterococci cells when exposed to light (negative is mortality)
Sinking	s	$m/\ day$	FL: 0 PA: 1	Sinking rate of particle-associated enterococci
Diffusivity	D	m^2/s	$0 \rightarrow 0.01$	Turbulent diffusivity, which simulates vertical mixing
Diffuse Attenuation Coefficient	K_d	m^{-1}	$0 \rightarrow 2$	The reduction of radiation by a factor of e; weakening of beam of light through water
Concentration	C	%		Amount of enterococci at a given point in time (set at 100% at t_0)

leaving an undisturbed 300-mL bottom layer, containing all particles that had settled by that time point.

Particle mass accumulated in the bottom layer at each time point was measured using volumetric subsamples filtered onto pre-weighed, combusted Whatman GF/F filters (25 mm diameter). A small volume of deionized water passed through the filter removed salts, and dried filters (100 °C for >24 h) were reweighed to calculate the total particle mass collected. Inorganic and organic particle masses were then estimated by Loss On Ignition (APHA, 2005) after combusting dried filters (450 °C for 4 h). Inorganic and organic particle concentrations in the bottom layers of successive settling columns were calculated for each time point and used to calculate the percent of initial particle mass that remained in suspension ($\left(1 - \frac{settled\ mass}{total\ mass}\right)$*100%) at each time point.

To distinguish particle-associated and free-living enterococci, a portion of the 300-mL bottom layer sample was processed for total enterococci, and a second subsample was passed through a 3-μm pore diameter membrane filter. Free-living enterococci were those that passed through the filter and the particle-associated fraction was calculated by subtraction from the total count. Quantifying enterococci of both fractions used Enterolert with Quanti-Tray/2000 (IDEXX Laboratories 2013) for most probable number.

Sinking rate estimation began by plotting the percent of each particle or enterococci fraction that remained suspended through time in successive settling columns (Owen, 1976; Aumack and Juhl, 2015). Best-fit curves, regressing the percent suspended against time, pooling data across experiments, were fit to each type of data. Statistical comparisons were based on the slopes of these best-fit regressions. The mean sinking velocity distribution for each type of particle was then calculated following Owen (1976), Jones and Jago (1996), and Malarkey et al. (2013).

2.2. 1-Dimensional persistence model

2.2.1. Model framework

To simulate the fate of enterococci in a 1-dimensional water column, we employed an advection-diffusion-decay framework that incorporated the empirically determined first-order growth rates. Consistent with previous studies (Fuchs et al., 2007; Rippy et al., 2013a, 2013b) vertical mixing was simulated via turbulent diffusivity (D) and impacted both fractions. Sinking (s), represented as vertical advection, only affected the particle-associated fraction. The general framework is represented by:

$$\frac{\partial C_{FL}}{\partial t} = D*\frac{\partial^2 C_{FL}}{\partial z^2} - \lambda_{FL}*C_{FL} \quad (1)$$

$$\frac{\partial C_{PA}}{\partial t} = D*\frac{\partial^2 C_{PA}}{\partial z^2} - s*\frac{\partial C_{PA}}{\partial z} - \lambda_{pa}*C_{PA} \quad (2)$$

where C_{FL} or C_{PA} = the concentration of free-living or particle-associated enterococci, D = turbulent diffusivity (meter^2/second), z = depth (meter), λ = total growth rate (second^{-1}), and s = sinking rate (meter/second). In these equations, both the light- and temperature-dependent growth rates were incorporated, as $\lambda_{FL\ or\ PA} = \sum \lambda_{light} + \lambda_{temperature}$. Simulations were run using a Forward-in-Time-Centered-in-Space (FTCS) Taylor Expansion with 1 s time steps for high temporal resolution. As an example, the FTCS for free-living enterococci not at the bottom or top boundary was:

$$C_{[t+1,z]} = D*\frac{\Delta t}{\Delta z^2}*\left(C_{[t,z+1]} - 2*C_{[t,z]} + C_{[t,z-1]}\right) + \left(1 + \Delta t*\left(\lambda_{light}(z)*Diel(t) + \lambda_{temp}\right)\right)*C_{[t,z]} \quad (3)$$

The *Diel(t)* function was a light curve multiplier for the light-induced loss parameter with a maximum value of 1 and minimum value of 0. *Diel(t)* was constrained as a sinusoidal function for 16 h and had a value of 0 for the subsequent 8 h to simulate a realistic diel cycle (e.g. summer at 45° latitude). The default scenario was for a discrete enterococci discharge occurring immediately prior to sunrise, without subsequent discharge. Discharge timing was manipulated in later simulation runs. Light-dependent growth rates (λ_{light}) throughout the water column were modeled similarly to diffuse light attenuation with depth (K_d), such that light-dependent growth was directly proportional to light level:

$$\lambda_{light}(z) = \lambda_{light}(0)*e^{(-K_d*z)} \quad (4)$$

where K_d = the diffuse attenuation coefficient of Photosynthetically Active Radiation (PAR) (meter^{-1}) and z = depth (meter). Note that we did not specify the wavelength for K_d, as the action spectrum for enterococci inactivation is not known. To simulate enterococci persistence in conditions that represent many water body types, the model was run over wide ranges of K_d (0–2 meters^{-1}, or infinite to 2.3 m depth of 1% light level) and D (0–0.01 meters^2/second) values that are consistent with literature values (Table 4).

At t = 0, the concentration of enterococci was 100%, which then advected, diffused, and decayed following the empirically determined parameters. We used T_{90}, defined as the time for 90% of the initial enterococci to decay, to compare across model runs and with previous studies (Kay et al., 2005; Brooks and Field, 2016). Concentrations were integrated throughout the water column and the first time point where $\sum_{Z=0\ m}^{Z=20\ m} C(z) \leq 10\%$ was T_{90}. The maximum T_{90} was set at 100 h, as other environmental factors, such as horizontal transport, would have a greater role in determining enterococci concentrations so long after introduction into a receiving water body. Accordingly, enterococci populations that would require over 100 h to decay to 10% and those increasing in concentration (i.e. growing), were assigned T_{90} = 100 h.

2.2.2. Sensitivity tests

Two different sensitivity tests addressed: 1) how sensitive is model output to changes in individual parameter values (growth and sinking rates)? and 2) given the observed variability in parameter values, how robust is the conclusion that particle association results in longer modeled enterococci persistence?

For the first question, one parameter (light- or temperature-dependent growth, or sinking rate) was allowed to vary, while other parameters were held constant at the experimentally-determined mean values, referred to as standard run values. K_d and D values in sensitivity tests were set to represent two environmentally-relevant extremes: a clear, quiescent lake (K_d= 0.087 m^{-1}, D = 1.34 *10^{-4}(meters^2/second)) using parameter values from Lake Tahoe (Abbott et al., 1984; Swift et al., 2006) and a turbid, turbulent estuary (K_d=2.0 m^{-1}, D = 0.01 (meters^2/second)) like the Hudson River Estuary (Stross and Sokol, 1989; Orton and Kineke, 2001). Using means and standard deviations of the empirical data, a vector of light-dependent and temperature-dependent growth rates with a normal distribution was generated. Light growth rates were represented as a truncated normal distribution, with values constrained to <0 (representing the assumption that light will not enhance enterococci growth). Sinking rates followed a gamma distribution of shape = 0.5 and scale 2. A vector of randomly-sampled rates from each distribution was generated and the mean and variances of each vector were compared to the empirical observations to ensure similarity. For each of the 1000 simulations per parameter and per fraction (6000 total simulation runs), a single growth or sinking rate was selected at random from this vector and then the model was run forward 96 h, with all other parameters held constant at standard run values. Sensitivity was quantified using the deviation (range-normalized, root mean squared deviation) of sensitivity test simulation runs from standard run values, yielding a measure of variability V in modeled T_{90} based on N variations of the empirically-determined parameters:

$$V = \sqrt{\left(\frac{\sum_{n=1}^{n=N}\left(T90(mean) - T90(n)\right)^2}{N}\right)} \Big/ \left(T90_{\max} - T90_{\min}\right) \quad (5)$$

A value of $V = 0$ would indicate that the model output is fully insensitive to changes in a given parameter.

A second set of sensitivity tests assessed the importance of particle association on enterococci persistence throughout the parameter space defined by variability in all empirically-measured parameters simultaneously. In the 1000 simulations per condition and per fraction for these tests, light- and temperature-dependent growth and sinking rates were all randomly selected from new vectors of the rates that had distributions similar to the empirical observations. Simulations were run for the lake and estuarine K_d and D conditions, with the difference in T_{90} between particle-associated and free-living fractions as the output. The distribution of these differences was then compared to simulations using standard value runs.

3. Results

3.1. Empirical rates

3.1.1. Dark, temperature-dependent growth rates

Environmental conditions for samples used in dark growth rate experiments are shown in Table A1. Table 2 shows mean dark growth rates of the free-living, particle-associated, and total enterococci at each experimental temperature. Raw data from each experiment are shown in Table A2. A two-way ANOVA with fraction (particle-associated vs. free-living) and temperature (5, 18, or 28 °C) as factors demonstrated a significant effect of fraction ($F_{1,30} = 6.48$, $p = 0.016$), but not temperature ($F_{2,30} = 0.58$, $p = 0.57$) on enterococci growth rates. *Post hoc* testing confirmed that the particle-associated fraction had significantly higher growth rates than the free-living fraction.

3.1.2. Light-dependent growth rates

Environmental conditions for samples used in light-dependent growth rate experiments are shown in Table A1. Raw data, incident light for normalization, and normalized light-dependent growth rates are shown in Table A3. Table 2 shows mean, normalized light-dependent growth rates for the free-living, particle-associated, and total enterococci at 18 °C. Light-dependent growth rates were all negative and 1–2 orders of magnitude larger than dark growth rates at the same temperature (previous section). Using an unequal variances, unpaired *t*-test, free-living and particle-associated light-dependent growth rates were found to be significantly different ($t_{11.9} = 2.4$, $p = 0.032$) from one another.

3.1.3. Sinking rates

Environmental conditions for samples used in sinking rate experiments are shown in Table A4. Inorganic and organic particles remaining in suspension declined significantly over time, with organic particles sinking significantly slower ($F_{1,50} = 28.24$, $p < 0.001$) (Fig. 1A). A similar analysis for particle-associated enterococci remaining in suspension (Fig. 1B), produced an exponential best fit with a significantly negative slope ($F_{1,\ 23} = 119.2$, $p < 0.0001$). In contrast, a linear regression applied to free-living enterococci indicated no significant change over time ($p = 0.12$). The best fit curves from Fig. 1A–B were used to estimate the mean sinking rate spectra of inorganic particles, organic particles, and particle-associated enterococci (Fig. 1C). Free-living cells did not sink appreciably during these experiments, while at least some particle-associated cells sank at rates greater than 1 m/day, though it is also likely that many particle-associated cells had negligible sinking rates.

3.2. Model results

3.2.1. Free-living enterococci $\boldsymbol{T}_{90}$ ($FL\boldsymbol{T}_{90}$)

Generally, FLT_{90} (i.e. persistence of free-living enterococci) increased with diffuse light attenuation (K_d) and turbulent diffusivity (D) (Fig. 2A). When turbulent diffusivity was near 0 (i.e. limiting vertical motion of free-living enterococci), variation in K_d had minimal impact on FLT_{90} ($\approx$1% increase). However, even slight increases in turbulent diffusivity above zero dramatically increased the effect of K_d on prolonging FLT_{90}. Meanwhile, for most values of K_d, increasing D prolonged FLT_{90}.

3.2.2. Particle-associated enterococci $\boldsymbol{T}_{90}$ ($PA\boldsymbol{T}_{90}$)

Patterns of PAT_{90} were similar to those of FLT_{90}, though for all combinations of K_d and D, PAT_{90} was longer (Fig. 2B). In addition, PAT_{90} was more sensitive to changes in K_d or D, in the sense that a given change in K_d or D increased PAT_{90} more than FLT_{90}. Above D = 5*10^{-6} meters^2/second, PAT_{90} often exceeded the model's maximum simulation time of 100 h, effectively reaching infinite persistence within the modeled domain (indicated by the pink color contour).

3.2.3. Difference in enterococci $\boldsymbol{T}_{90}$ ($\Delta\ \boldsymbol{T}_{90}$)

The difference in simulated T_{90} of each fraction ($\Delta T_{90} = PAT_{90} - FLT_{90}$) was consistently greater than 0, indicating that particle-

Table 2
Growth Rates. Summary data from dark, temperature-dependent and light-dependent growth rate experiments, separated for each fraction.

Parameter	Temp (°C)	Free-Living (day^{-1})	Std Dev	Particle-Associated (day^{-1})	Std Dev	Total (day^{-1})	Std Dev
λ_{Temp}	5	0.013	0.241	0.301	0.664	0.057	0.280
	18	−0.359	0.522	0.331	0.624	−0.110	0.229
	28	−0.287	0.446	0.135	0.674	−0.157	0.446
λ_{Light}	18	−33.314	19.496	−16.478	6.259	−29.926	20.935

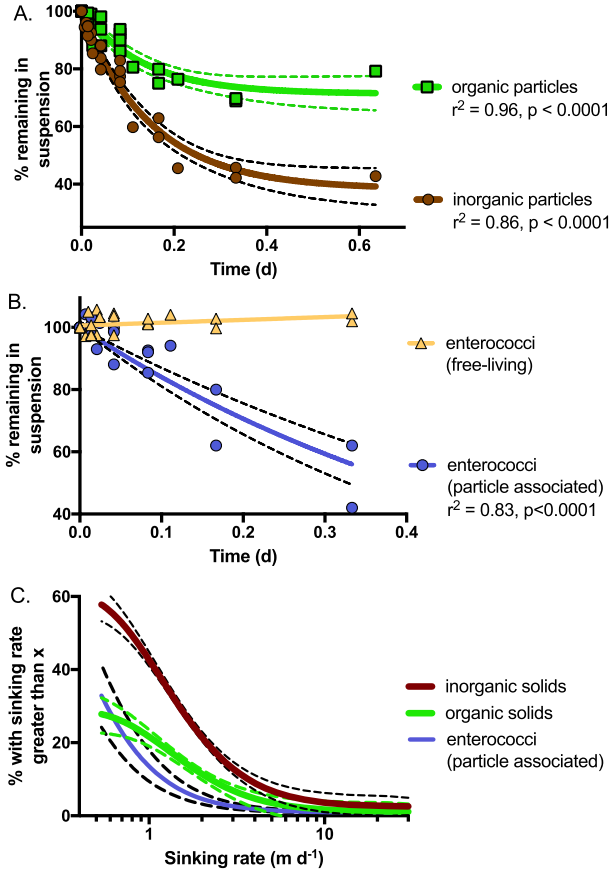

Fig. 1. Empirical sinking rate data.
Data from sinking rate experiments conducted using water collected from the HRE. Percent of initial suspended particles (inorganic and organic) remaining in suspension at each time point (A). Percent of initial particle-associated and free-living enterococci remaining in suspension at each time point (B). Solid lines in (A) and (B) are the best-fit curves for data pooled across 5 experiments, dashed curves indicate the 95% CI of each curve. Distribution of sinking rates (solid curves) and 95% CI (dashed curves) were calculated using the regressions shown in (A) and (B) (C). The curves indicate the particle population fraction with a sinking rate greater than the value shown by the respective curve. For example, approximately 43% of the inorganic particles, 22% of the organic particles and 14% of the particle-associated enterococci had sinking rates >1 m/day.

associated enterococci persisted longer than free-living enterococci in standard simulation runs at all values of K_d and D (Fig. 2C). The difference in persistence between fractions ranged 1.7–96 h (1.5–13 x greater). The difference between fractions was minimized overall when K_d or D were near zero. The difference between fractions was also most sensitive to changes in K_d when D was low. Specifically, under low to moderate D ($0 - 5*10^{-5}$ $meters^2/second$), PAT_{90} increased more (up to 15x greater) than FLT_{90} (up to 6.5 x greater), as K_d increased from 0 to 2 $meter^{-1}$. At higher D values, changes in K_d had less effect on the difference between fractions. The greatest difference in T_{90} between fractions (blue contour, Fig. 2C) occurred with low D and moderate to high K_d values. A region of similar difference also extended throughout the diffusivity range at moderate K_d values.

3.2.4. Diel cycle effects on enterococci T_{90}

In addition to the default discharge immediately prior to sunrise presented above, simulations were run with inputs of enterococci occurring at different times throughout the 16-h day and 8-h night cycle. Simulated discharges occurring later in the day consistently increased T_{90} of both free-living and particle-associated fractions (Fig. 3, Figs A3 and A4), relative to the default discharge scenario (sunrise, Fig. 2), with the greatest difference for discharge at 16 h (sunset, Fig. 3). Simulated discharge at 16 h increased the minimum simulated T_{90} for both free-living (4.6 to 12.5 h) and particle-associated (6.4 to 14.5 h) fractions. Later discharges had a greater effect on FLT_{90} than on PAT_{90}, particularly in regions of moderate to high K_d and low diffusivity. In general, FLT_{90} was more variable across the range of K_d and D values and over various discharge times than PAT_{90}. Therefore, patterns in the ΔT_{90} plots primarily reflect the patterns of FLT_{90}.

3.2.5. Sensitivity tests

The first set of sensitivity tests, that examined model sensitivity to changes in one set of rates at a time, demonstrated a greater sensitivity (i.e. increased variability, V) of T_{90} to dark, compared to light-dependent, growth rates. In addition, FLT_{90} was more sensitive to rate changes than PAT_{90}, and sensitivity of both fractions was greater for the higher K_d and D values representing estuarine conditions, compared to the simulations representing a clear, quiescent lake (Fig. 4). For example, allowing dark growth rates to vary under the estuarine conditions generated greater V for FLT_{90} ($V = 0.33$) than PAT_{90} ($V = 0.24$). Variability in T_{90} values was lower in sensitivity tests using the clear, quiescent lake conditions, though changes in dark growth rates still caused more variability in FLT_{90} ($V = 0.145$) than in PAT_{90} ($V = 0.139$).

Allowing light-dependent growth rates to vary had the greatest impact on FLT_{90} under estuarine conditions ($V = 0.248$), though persistence of the particle-associated fraction was always infinite in those conditions, resulting in 0 computed variability within the sensitivity runs. In lake conditions, free-living ($V = 0.081$) and particle-associated ($V = 0.070$) persistence was relatively insensitive to varying light-dependent growth rates (Fig. 4).

Only PAT_{90} under lake conditions was measurably sensitive to varying sinking rates ($V = 0.0897$), as PAT_{90} in turbid, turbulent estuarine conditions consistently reached the maximum (or infinite) T_{90} values, regardless of sinking rate. The simulated free-living fraction did not sink, so FLT_{90} values did not change with different sinking rates.

In the second set of sensitivity tests, where all rates were allowed to vary between successive simulation runs, PAT_{90} was greater than FLT_{90} for 80.7% of lake trials and for 88.5% of estuarine trials. In some runs, T_{90} of both fractions exceeded 100 h. Because of the negative mean dark growth rates for free-living vs. positive mean dark growth rates of particle-associated enterococci, trials with T_{90} of both fractions exceeding 100 h ($\Delta T_{90} = 0$) were counted towards greater

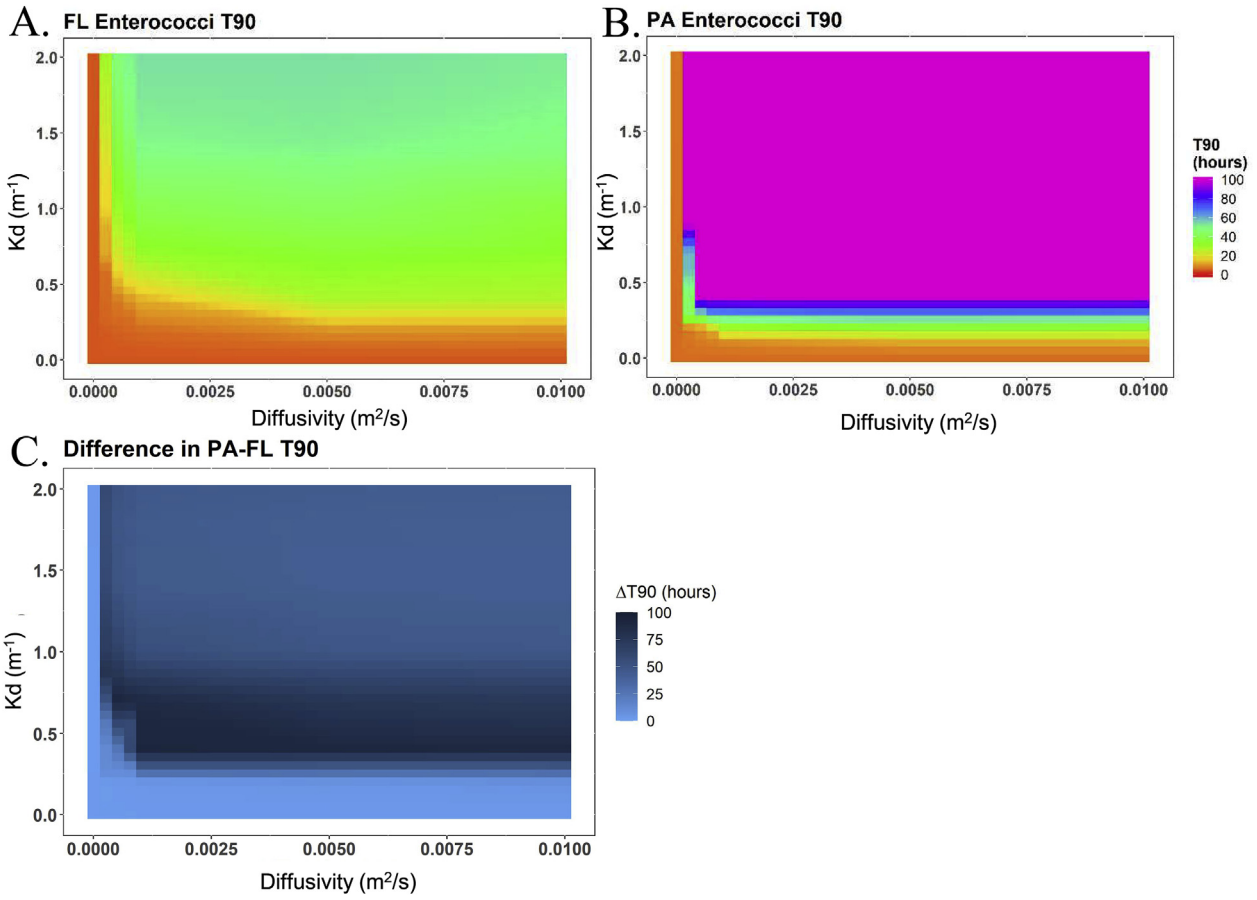

Fig. 2. Standard model run T_{90}.
Simulated persistence (T_{90}) is shown for free-living (A) and particle-associated (B) enterococci under the default discharge scenario (at sunrise) for standard run values. Color bar indicates T_{90}, the time it takes for 90% of enterococci to decay. T_{90} is plotted against a wide, physically relevant range of K_d (diffuse attenuation coefficient) and Diffusivity. The difference in T_{90} between particle-associated and free-living enterococci (B–A) is always greater than 0 (C).

persistence by the particle-associated fraction in the percentages given above. FLT_{90} and PAT_{90} were more sensitive to rate changes under estuarine ($V = 0.35$ and $V = 0.28$, respectively) than lake ($V = 0.09$ and $V = 0.12$, respectively) conditions. Also, using equation (5) for ΔT_{90}, sensitivity of ΔT_{90} values to rate changes was lower for the lake vs. estuarine conditions ($V = 0.073$ and 0.243, respectively).

4. Discussion

4.1. Empirically-determined growth and sinking rates

While numerous studies have quantified growth or decay rates of enterococci and other FIBs, this is the first study to separately quantify growth rates for particle-associated and free-living enterococci populations. The higher light-dependent and dark growth rates of particle-associated vs. free-living enterococci are consistent with arguments that particles provide a more favorable environment for bacteria, including FIB. The two fractions also differed because particle-associated enterococci had measurable sinking rates, while the free-living fraction remained suspended. These quantitative differences in rates that are critical for FIB ecological dynamics in receiving water bodies highlight the important distinctions between these two fractions.

4.1.1. Dark, temperature-dependent growth

The temperature dependence of mean dark growth rates measured in this study for the total fraction of enterococci was consistent with previous empirical studies. Many studies have reported more negative dark growth rates at high temperatures and growth rates closer to 0 per day at low temperatures (Craig et al., 2002; Noble et al., 2004; Boehm et al., 2018). Further, greater persistence of FIB observed in winter than summer (Maïga et al., 2009; Maraccini et al., 2016; Ballesté et al., 2018) has been partially attributed to lower temperatures. However, our results demonstrate that temperature-dependence of total fraction growth rates in our experiments was primarily driven by the free-living fraction, as mean particle-associated enterococci growth rates were more consistent across the temperature range. Note that mean dark growth rates of the particle-associated fraction were positive at every temperature, while those of the free-living fraction became negative at higher temperatures. Therefore, some of the variability of temperature-dependent growth rates in previous studies may be due to the variable degree of particle association of FIB in the population studied. Based on results of this study, dark growth rates measured for a predominantly free-living population of enterococci could show greater temperature dependence and overall be more negative, while less temperature dependence and even positive growth rates could be found in a population of enterococci that was predominantly particle-associated.

Dark growth rates of total enterococci measured in this study were also comparable to the means and variability reported in other studies at similar temperatures (Table 3). In our data, mean dark growth rates were towards the higher end of the range of values at each temperature presented in Table 3, implying longer

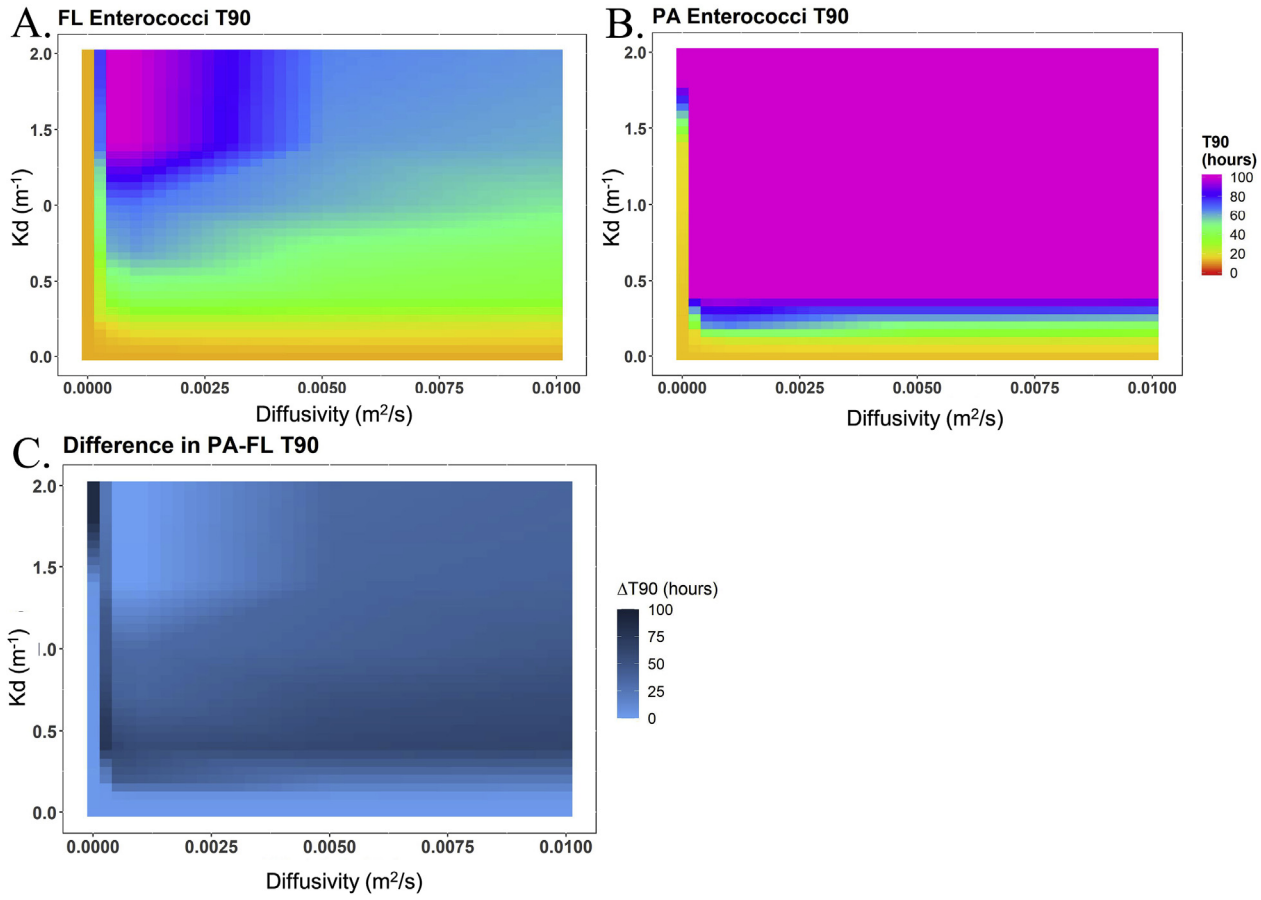

Fig. 3. Later discharge model run T_{90}.
Simulated persistence, T_{90}, for free-living (A) and particle-associated (B) enterococci is shown using standard run values and a discharge time of 16 h, immediately prior to sunset. T_{90}values are shown via color bar and are plotted along a wide range of K_d (diffuse attenuation coefficient) and Diffusivity. The difference in T_{90} for particle-associated and free-living enterococci (B–A) is consistently greater than 0 (C).

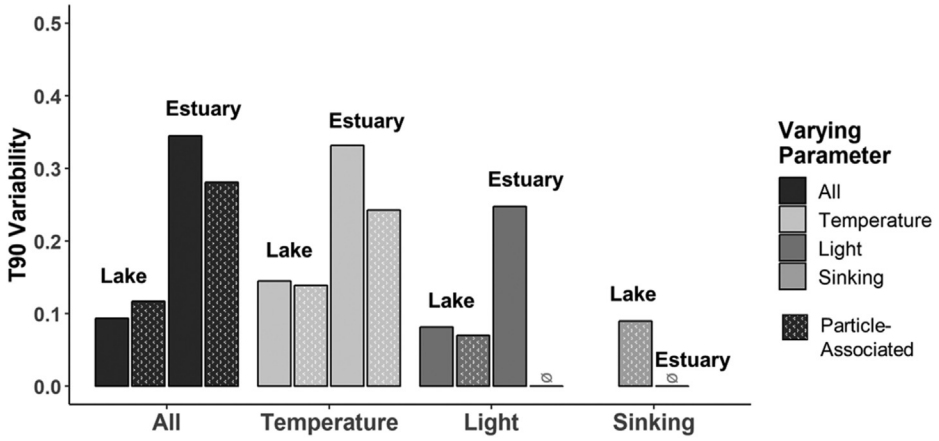

Fig. 4. Model variability from rate manipulation.
Model variability (V), measured by comparing standard run value model outputs to 1000 different runs per sensitivity test (calculated using the range-normalized, root mean squared deviation formula, equation 5), is plotted against each sensitivity test. Outputs are grouped according to which rates were manipulated over the 1000 simulations: all rates, temperature-dependent growth, light-dependent growth, or sinking. Variability outputs are labeled to denote if tests were performed for approximated lake or estuary conditions. Particle-associated predictions are denoted by stippling. Sensitivity tests where all simulations resulted in T_{90} > 100 h are denoted by the symbol Ø.

persistence. This was most notable at 5 °C, where all fractions of enterococci experienced positive growth, contrary to the low negative growth for FIB commonly observed at this temperature (e.g. Evison, 1988; Menon et al., 2003). Positive extra-enteric growth of enterococci has been observed in sediments (e.g. Jeng et al., 2005; Yamahara et al., 2009), in association with organic rich substrates, such as algae and vegetation (e.g. Byappanahalli et al., 2003; Byappanahalli and Whitman, 2009; Imamura et al.,

Table 3
Survey of Empirically-Determined Enterococci Growth Rates. A summary table of dark and light-dependent enterococci growth rates with temperature, enterococci source, and matrix distinction. Rates (day^{-1}) are reported as: mean (standard deviation, when available).

Experiment	Paper	Temperature (°C)				Enterococci Source	Matrix
Light		4–10	14	15–20	25–30		
Dark	Suter and Juhl 2008[a]	−0.02 (0.11)		−0.17 (0.22)	−0.83 (0.41)	cultured enterococci	Hudson River water
Dark				−0.80 (0.51)		cultured enterococci	Hudson River water
Dark				−0.22 (0.11)	−0.14 (0.03)	cultured enterococci	NY Harbor water
Dark	Jeng (2005)				−0.18	cultured enterococcus faecalis	"estuarine water"
Dark	Noble (2004)		−0.38 (0.12)	−0.46 (0.10)		Urban runoff (storm drain)	seawater
Dark			−0.48 (0.14)	−0.31 (0.12)		raw effluent WWTP	seawater
Dark	Craig (2002)	−0.26 (0.11)		−0.41 (0.24)	−1.01 (0.97)	cultured enterococci	seawater
Dark	Sinton et al. (2002)		−0.40 (0.10)			waste stabilization pond (WSP) effluent	WSP
Dark			−0.29 (0.05)			raw sewage	freshwater
Dark	Sinton (1994)	−0.12 (0.09)		−0.19 (0.01)		sewage effluent	seawater
Full Sun	Mattioli (2017)			−3.90 (0.65)		cultured enterococci	seawater
Full Sun	Maracinni (2016)			−3.90 (0.38)		raw sewage	seawater
					−2.75 (0.20)	raw sewage	freshwater
Full Sun	Juhl 2009[a]			−13.8 (2.5)		Hudson River Estuary (in situ)	estuarine water
Full Sun	Suter and Juhl 2008[a]			−26.1 (0.21)		cultured enterococci	estuarine water
10% Sun				−5.5 (1.1)		cultured enterococci	estuarine water
High	Noble (2004)			−6.17 (0.18)		raw effluent source	seawater
Low				−5.84 (0.53)		raw effluent source	seawater
High				−6.54 (0.16)		raw effluent source	freshwater
Low				−5.84 (−.32)		raw effluent source	freshwater
Full Sun	Sinton (2002)		−3.14			raw sewage	freshwater
			−3.72			raw sewage	simulated estuarine water
			−4.73			raw sewage	seawater
			−5.38			waste stabilization pond (WSP) effluent	freshwater
			−5.59			waste stabilization pond (WSP) effluent	simulated estuarine water
			−7.34			waste stabilization pond (WSP) effluent	seawater
Cloudy Sky			−5.02			raw sewage	freshwater
			−4.54			raw sewage	simulated estuarine water
			−8.11			raw sewage	seawater
			−5.45			waste stabilization pond (WSP) effluent	freshwater
			−6.70			waste stabilization pond (WSP) effluent	simulated estuarine water
			−7.54			waste stabilization pond (WSP) effluent	seawater
Full Sun	Davies-Colley (1994)		−40.90			sewage effluent	seawater
Low Cloud	Sinton (1994)	−4.61				raw sewage effluent	seawater
Clear to Cloudy			−8.63			raw sewage effluent	seawater

[a] Denotes unpublished data.

2011), and in treated wastewater with high dissolved nutrients (Surbeck et al., 2010). Therefore, our relatively high growth rates could be related to high levels of dissolved organic matter in the Hudson River (Findlay, 2005).

Similarly, higher substrate availability on particles could contribute to the elevated dark growth rates of particle-associated vs. free-living enterococci. Because dark growth rates aggregate numerous ecological and physiological processes, other potential advantages of particle association (Davies and Bavor, 2000; Craig et al., 2002; Hess-Erga et al., 2008) may also drive differences in dark growth rates observed between the two fractions. In any case, our data support the hypothesis that particle association benefits enterococci survival, similar to results reported for particle-associated *E. coli* (Garcia-Armisen and Servais, 2009). Furthermore, positive growth for the particle-associated fraction of enterococci contradicts the general assumption that the extra-enteric ecology of FIB populations is dominated by loss. It remains an open question if other sewage-derived bacteria have similar particle association and ecological dynamics.

4.1.2. Light-dependent growth

Consistent with previous studies, enterococci growth rates under sunlight exposure were significantly more negative than dark growth rates. The mean and variance of light-dependent growth rates of total enterococci observed in this study fall within ranges reported in the literature (Table 3). High variability of reported rates within and between studies is unsurprising, as different factors can interact with light to alter light-induced inactivation rates (Davies-Colley et al., 1994; Maïga et al., 2009; Yeh et al., 2011). Furthermore, our study is based on short experiments during maximum sunlight exposure and minimal cloud cover, so the rates we report are likely the maximum for the day.

The more negative light-dependent growth rates of free-living enterococci in this study are consistent with size fractionation studies that report the most negative FIB light-dependent growth rates for the smallest size fractions, which include free-living cells (Qualls et al., 1983; Madge and Jensen, 2006; Walters et al., 2014). Differing growth rates reported for various size fractions could relate to differences in shading efficacy. However, we cannot resolve the mechanism responsible for the higher mean light-dependent growth rates of particle-associated vs. free-living enterococci from our experiments, indicating future research is warranted.

4.1.3. Sinking rate distribution

Direct observations of FIB sinking rates are rare, but the reported range of 0.5–1.6 m/day for particle-associated fecal coliforms and *E. coli* (Auer and Niehaus, 1993; Garcia-Armisen and Servais, 2009) encompasses particle-associated enterococci sinking rates found in this study. Some modeling studies have used ideal calculations of particle deposition and resuspension (Steets and Holden, 2003; Sanders et al., 2005) or Stokes' law (Cho et al. 2010) for estimating sinking of FIB. Much higher particle-associated FIB sinking rates have been estimated in streams where the particles are

predominantly resuspended sediment (Jamieson et al., 2005a). Particle size preference of FIB likely influences sinking rates. FIB sinking rates that are slow relative to the rest of the particle field, like in this study, suggest dominant FIB attachment to smaller particles. Previous studies have often found FIB to be more frequently associated with fine sediments and particles (Davies and Bavor, 2000; Jamieson et al., 2004; Walters et al., 2014), though not always (Mote et al., 2012). Particle composition also very likely plays a role in altering sinking rates through particle density and structure. By assessing a sinking rate distribution rather than a mean rate, this study encompasses some of the variability in enterococci sinking due to particle composition. Further research on particle size or type preference of sewage microbes would better constrain sinking rates that should be used in models of FIB persistence.

4.2. Simulated persistence of particle-associated and free-living enterococci

Recent FIB modeling studies cite a lack of confidence in parameterizing distinct growth rates for particle-associated and free-living FIB. This is the first modeling study to 1) incorporate empirically-quantified, distinct growth rates for particle-associated and free-living enterococci and, 2) simulate how variation in light exposure with time of day and depth could affect FIB persistence. Results of these simulations demonstrate distinct ecological dynamics for particle-associated vs. free-living enterococci, stemming from quantitative differences in critical rates, which supports measuring the two fractions as distinct populations and considering the impacts of FIB particle association in water quality management.

4.2.1. Modeled dark growth

Many models represent FIB growth via background rates that depend on temperature (Neitsch et al., 2009; Hipsey et al., 2008; Kim et al., 2010; Niazi et al., 2015), and sometimes salinity (Chen and Liu, 2017). Our total enterococci growth rates support the former, though temperature influenced dark growth rates less than particle association. Salinity impacts were not included in our model because we found no impact of salinity in our experiments and literature reports of the impact of salinity are inconsistent, suggesting lower enterococci sensitivity to salinity than other FIB (Noble et al., 2004; Anderson et al., 2005).

4.2.2. Modeled light-dependent growth

Some previous FIB models have highlighted the importance of light effects on FIB growth rates, including light variability due to day vs. night, sunlight intensity, depth, and water column turbidity (Auer and Niehaus, 1993; Hellweger and Masopust, 2008; Cho et al., 2010; Gao et al., 2015). However, light-dependence was also omitted, or not explicitly incorporated, in other previous modeling studies (Russo et al., 2011; Chen and Liu, 2017; Wen et al., 2017), at least partly due to insufficient data. Including variable light-dependent growth rates improved model validation against field data in some cases (Cho et al., 2010), though not in others (Hellweger and Masopust, 2008; Rippy et al., 2013a). In Rippy et al. (2013a) the lack of impact of varying light-dependent growth rates on model outputs could be due to the relatively short study duration (5 h sunlight exposure), while Hellweger and Masopust (2008) argued that their model may have been biased by using a single water column K_d throughout their study region. Our simulations indicated that varying K_d notably altered FIB persistence, supporting the argument that use of a single K_d value could weaken model validation against field data. Moreover, the combined dependence in our model of light-dependent growth rates on time of day, light attenuation, and depth in water column underscored the importance of including variability of light in FIB persistence predictions.

4.2.3. Distinguishing particle-associated and free-living enterococci

Incorporation of subpopulations with different growth rates, as in this study, is rare in FIB models. Uniform growth rate parameters are commonly imposed across total FIB populations (Hipsey et al., 2008; Coffey et al., 2010; Bougeard et al., 2011; Pandey et al., 2016), though some models have simulated FIB populations of differential persistence (Sadeghi and Arnold, 2002; Hellweger and Masopust, 2008; Bucci et al., 2012; Rippy et al., 2013b) or distinguished particle-associated and free-living FIB (de Brauwere et al., 2014; Chen and Liu, 2017). When included in FIB fate models, particle association is primarily linked to transport processes, like resuspension and deposition to the sediments (R. C. Jamieson et al., 2005; R. Jamieson et al., 2005; Yang et al., 2008; Cho et al., 2010; Kim et al., 2010; Feng et al., 2016), though deBrauwere et al. (2014) included a positive impact of particle association on growth rates of *E. coli*. The divergent persistence between independently parameterized particle-associated and free-living fractions in our simulations suggests that future FIB modeling studies should distinguish these subpopulations, whether or not sediment resuspension is incorporated within the model.

4.2.4. Simulated impacts of K_d and D on persistence

In our model, K_d and D, reflective of literature values (Table 4), control enterococci persistence, as all fractions can be transported vertically via turbulent motion (D) and particle-associated cells also sink, both processes that alter light exposure in accordance with K_d. Because solar inactivation of FIB is caused by both UV and visible light (Fujioka et al., 1981; Davies-Colley et al., 1994; Sinton et al., 2002), K_d values in these simulations can be contextualized by comparisons to K_d PAR. However, the conclusions of this study are not based on wavelength-specific K_d, and predictions for any wavelength band could be extracted by selecting an appropriate K_d value. In our simulations, high K_d values lowered the effect of light exposure on growth rates at each depth, making net growth rates more dependent on dark growth rates. These trends are consistent with experiments demonstrating that light-dependent growth rates of enterococci are less negative with increasing turbidity (Alkan et al., 1995; Whitman et al., 2004; Kay et al., 2005; Gutiérrez-Cacciabue et al., 2016) and that rates in turbid water were similar to dark growth rates (Kay et al., 2005). In addition, the proportionality of light-dependent growth rates in our model as light exposure changes due to depth and time of day is supported by commensurate changes in FIB growth rates with varying light exposure due to turbidity (Kay et al., 2005), depth (Davies-Colley et al., 1994), and exposure time (Auer and Niehaus, 1993; Sinton et al., 2002).

Turbulence, as represented by D, primarily affected enterococci persistence in our model by impacting their depth distribution, which altered light exposure according to K_d. Our simulations suggest interactive effects of K_d and D as seen by the greater increase in T_{90} (of both fractions) when K_d and D increased together, as opposed to separately. Impacts of turbulence on enterococci growth rates or water column concentrations in previous studies have also been linked to changes in turbidity (Palmateer et al., 1989; Whitman et al., 2004), demonstrating empirical support for an interaction between turbulence and turbidity on FIB. Direct effects of turbulence on FIB growth rates have been suggested (Al-Homoud and Hondzo, 2008), though are not included in this model. Vertical mixing has also been previously connected to increased water column concentrations of FIB through resuspension of sediment-bound FIB (Steets and Holden, 2003; Craig et al., 2004). While the source potential of longer persisting enterococci at depth is acknowledged in our model by the mixing up from deeper layers of

Table 4
Survey of Empirically-Determined Diffuse Attenuation and Diffusivity Values. A summary table of values of diffuse attenuation of light coefficients (Kd) and turbulent diffusivity values (D) reported from different water body types. Units for Kd are m^{-1} and units for D are m^2/s.

Parameter	Paper	Value m^{-1} OR m^2/s	Sample Type	Location
Kd 420 nm	Morel et al. (2007)	0.012	open ocean	South Pacific gyre
Kd 400–590 nm	Tyler, ed. (1973)	0.025	open ocean	Sargasso Sea
Kd PAR	unpublished; in Austin and Petzold (1986)	0.043–0.227	coastal & offshore ocean	California Bight
Kd PAR	Rose et al. (2009)	0.066	oligotrophic lake	Lake Tahoe
Kd PAR	Lund-Hansen (2004)	0.152–0.557	sea/estuarine transition	North Sea-Baltic Sea estuarine transition
Kd PAR	Stross and Sokol (1989)	2.02	estuarine system (average)	Hudson River Estuary
Kd PAR	Cole et al. (1992)	1–2, 4	estuarine system	Hudson River Estuary (summer, winter)
Kd PAR	Carter and Rybicki (1990)	1.5–4	estuarine system	Potomac River & Estuary
Kd 470 nm	Champ et al. (1980)	2.44	estuarine system	Chesapeake Bay
Diffusivity	Toole et al. (1994)	$1*10^{-5}$	ocean background internal wave field	abyssal NE Pacific & NE Atlantic Ocean
Diffusivity	Quay et al. (1980)	$5*10^{-9}$– $1.7*10^{-7}$	lake	ELA Lake 227
Diffusivity		$8*10^{-8}$ – $1.8*10^{-6}$	lake	ELA Lake 224
Diffusivity	Wodka et al. (1983)	$6*10^{-6}$	lake	Onondaga Lake (early summer)
Diffusivity		$2*10^{-7}$	lake	Onondaga Lake (late summer)
Diffusivity	Geyer and Signell (1992)	$2*10^{-3}$ – $6*10^{-2}$	estuarine	general bays & estuaries estimate
Diffusivity	Orton and Kineke (2001)	$5*10^{-3}$– $3*10^{-2}$	estuarine	Hudson River Estuary (calculations)
Diffusivity	Stacey et al. (1999)	$2*10^{-2}$	bay	San Francisco Bay (rapid mixing event)

both fractions, we did not explicitly include deposition or resuspension from sediments.

At every value of K_d and D in the standard run simulations, particle-associated enterococci persisted longer than free-living enterococci. Minimal ΔT_{90} corresponded to when K_d or D were close to 0, reflecting clear and/or quiescent conditions, while greater ΔT_{90} corresponded to higher K_d and D, representing more turbid and/or turbulent waters. Variation in ΔT_{90} between fractions predominantly reflected patterns of FLT_{90} and was greatest at the transitions from low to moderate values of both K_d and D. It is worth noting that the sharp contrast surrounding the regions of maximal ΔT_{90} (transition from dark blue to lighter blue contours in the upper portion of Fig. 2C) is partially due to the imposed maximum T_{90} value of 100 h in these simulations. Had simulations been run longer, the dark blue region of maximum difference would likely extend further along the axis of increasing K_d.

4.2.5. Simulated diel cycle effects on persistence

In urban areas, where FIB abundance is dominated by intermittent point source discharges (e.g. combined sewer overflows), sewage discharges can occur at different times throughout the diel cycle, with correspondingly altered light exposure for discharged FIB. In this study, persistence for both fractions increased for simulated discharges occurring closer to sunset (16 h), due to the interaction between turbulence and light exposure. For example, simulated discharges at sunset (16 h) allowed a portion of both enterococci fractions to be transported deeper in the water column before sunrise, decreasing cumulative light-induced inactivation and increasing T_{90} values by at least 24 h (compared to modeled sunrise discharge). Simulated free-living enterococci benefited the most from mixing during dark period hours. The greatest increase in simulated FLT_{90} occurred at low to moderate D and high K_d, when some cells were transported into low-light, deep layers. As in the sunrise discharge scenario, at high D, vertical transport increased cumulative light exposure of simulated enterococci and decreased persistence. Results from these simulations suggest that discharge timing within a diel cycle may be an important factor in predicting enterococci persistence. Future FIB studies could include high frequency sampling within a diel cycle to test this hypothesis against field measurements.

4.3. Model sensitivity testing

In model sensitivity tests, FLT_{90} was generally more variable than PAT_{90}, and simulated estuarine conditions led to greater FLT_{90} variability than in the lake simulations. Higher variability under estuarine conditions was due to the steeper vertical gradient in light exposure with depth than in the lake conditions. One caveat to these tests was that variability in PAT_{90} was not calculated for the estuarine simulations because the time scale exceeded 100 h. Nevertheless, in both estuarine and lake conditions, 80–90% of simulations from the second set of sensitivity tests, where all rates were allowed to vary, resulted in greater persistence of particle-associated than free-living enterococci. The consistency of this result across wide parameter ranges strongly supports the hypothesis that particle association can prolong FIB environmental persistence.

In general, of the parameters manipulated in sensitivity testing, our model was most sensitive to changes in dark growth rate. However, the lower model sensitivity to variable light-dependent growth rates does not indicate a lack of importance of these rates for predicting persistence. In simulations where light-dependent growth rates were omitted from our model, T_{90} was 100+ hours for both fractions throughout the range of K_d and D (data not shown). Similarly, the importance of light-dependent growth rates on persistence is shown by the effect of K_d on T_{90} patterns of both fractions. Sinking rates only affected the particle-associated fraction and, under the lake conditions, resulted in PAT_{90} variability that fell between light and dark PAT_{90} variability. Sinking rate sensitivity tests, therefore, suggest that empirically well-constrained sinking rates are more important for predicting particle-associated FIB persistence under lake compared to estuarine conditions. Overall, simulations in which sinking rate was omitted led to similar T_{90} predictions of particle-associated enterococci, except at relatively low K_d and D conditions (Fig. A5). Sensitivity tests where all rates were modified resulted in variability similar to sensitivity tests where only dark growth rates varied, underscoring the relative importance of quantifying dark growth rates for modeling FIB persistence.

5. Conclusions

Particle association of enterococci increased critical growth rates and induced sinking, leading to longer simulated persistence of the particle-associated vs. free-living fraction across a wide range of physically-relevant values of diffuse light attenuation and turbulent diffusivity. Future experiments could especially focus on constraining fraction-specific dark, temperature-dependent growth rates, due to the high sensitivity of simulated persistence

to this rate. The generally higher sensitivity of simulated persistence to changes in all rates in the estuarine scenario suggests that empirical rate determination is especially critical in turbid and turbulent water bodies. Further, increased simulated persistence of both enterococci fractions with discharges later in the day suggests that further research should examine the effects of sewage discharge time within the diel cycle on downstream FIB persistence. The important role of particle association in the extra-enteric ecology of enterococci persistence revealed in this study suggests that future research should assess the impacts of particle association for other sewage-derived microbes, especially potential pathogens that pose human health risks.

Funding sources

This work was supported by the U.S. National Aeronautics and Space Administration through the Future Investigators in Earth & Space Science & Technology program [grant number 80NSSC19K1370]. Additional funding was provided by Riverkeeper, Inc.

Declaration of competing interest

The authors declare that they have no known competing financial interests or personal relationships that could have appeared to influence the work reported in this paper.

Acknowledgements

The authors would like to thank Carol Knudson and Captain John Lipscomb for assisting in field sample collection and Simon Levin for early conversations about model development. The authors would like to express their appreciation to the anonymous reviewers, whose comments greatly improved this manuscript. LDEO contribution #8437.

Appendix A. Supplementary data

Supplementary data to this article can be found online at https://doi.org/10.1016/j.watres.2020.116140.

References

Abbott, M.R., Denman, K.L., Powell, T.M., Richerson, P.J., Richards, R.C., Goldman, C.R., 1984. Mixing and the dynamics of the deep chlorophyll maximum in Lake Tahoe 1: chlorophyll dynamics. Limnol. Oceanogr. 29 (4), 862–878. https://doi.org/10.4319/lo.1984.29.4.0862.

Ahmed, W., Gyawali, P., Sidhu, J.P.S., Toze, S., 2014. Relative inactivation of faecal indicator bacteria and sewage markers in freshwater and seawater microcosms. Lett. Appl. Microbiol. 59 (3), 348–354. https://doi.org/10.1111/lam.12285.

Ahn, J.H., Grant, S.B., Surbeck, C.Q., DiGiacomo, P.M., Nezlin, N.P., Jiang, S., 2005. Coastal water quality impact of stormwater runoff from an urban watershed in Southern California. Environ. Sci. Technol. 39 (16), 5940–5953. https://doi.org/10.1021/es0501464.

Al-Homoud, A., Hondzo, M., 2008. Enhanced uptake of dissolved oxygen and glucose by Escherichia coli in a turbulent flow. Appl. Microbiol. Biotechnol. 79 (4), 643–655. https://doi.org/10.1007/s00253-008-1446-x.

Alkan, U., Elliott, D.J., Evison, L.M., 1995. Survival of enteric bacteria in relation to simulated solar radiation and other environmental factors in marine waters. Water Res. 29 (9), 2071–2080. https://doi.org/10.1016/0043-1354(95)00021-C.

Anderson, K.L., Whitlock, J.E., Harwood, V.J., 2005. Persistence and differential survival of fecal indicator bacteria in subtropical waters and sediments. Appl. Environ. Microbiol. 71 (6), 3041–3048. https://doi.org/10.1128/AEM.71.6.3041-3048.2005.

APHA, A., 2005. Standard Methods for the Examination of Water and Waste-Water. WEF, pp. 2–58, 2–61.

Appiani, E., McNeill, K., 2015. Photochemical production of singlet oxygen from particulate organic matter. Environ. Sci. Technol. 49 (6), 3514–3522. https://doi.org/10.1021/es505712e.

Auer, M.T., Niehaus, S.L., 1993. 'Modeling fecal coliform bacteria—I. Field and laboratory determination of loss kinetics'. Water Res. 27 (4), 693–701. https://doi.org/10.1016/0043-1354(93)90179-L.

Aumack, C.F., Juhl, A.R., 2015. Light and nutrient effects on the settling characteristics of the sea ice diatom Nitzschia frigida: light and nutrient effects on settling rates. Limnol. Oceanogr. 60 (3), 765–776. https://doi.org/10.1002/lno.10054.

Austin, R.W., Petzold, T.J., 1986. Spectral dependence of the diffuse attenuation coefficient of light in ocean waters. Opt. Eng. 25 (3), 253471. https://doi.org/10.1117/12.7973845.

Ballesté, E., García-Aljaro, C., Blanch, A.R., 2018. Assessment of the decay rates of microbial source tracking molecular markers and faecal indicator bacteria from different sources. J. Appl. Microbiol. 125 (6), 1938–1949. https://doi.org/10.1111/jam.14058.

Banas, N.S., Conway-Cranos, L., Sutherland, D.A., MacCready, P., Kiffney, P., Plummer, M., 2015. Patterns of river influence and connectivity among subbasins of Puget Sound, with application to bacterial and nutrient loading. Estuar. Coast 38 (3), 735–753. https://doi.org/10.1007/s12237-014-9853-y.

Bedri, Z., Bruen, M., Dowley, A., Masterson, B., 2011. A three-dimensional hydro-environmental model of dublin bay. Environ. Model. Assess. 16 (4), 369–384. https://doi.org/10.1007/s10666-011-9253-7.

Bienfang, P., Laws, E., Johnson, W., 1977. Phytoplankton sinking rate determination: technical and theoretical aspects, an improved methodology. J. Exp. Mar. Biol. Ecol. 30 (3), 283–300. https://doi.org/10.1016/0022-0981(77)90037-5.

Boehm, A.B., Graham, K.E., Jennings, W.C., 2018. Can we swim yet? Systematic review, meta-analysis, and risk assessment of aging sewage in surface waters. Environ. Sci. Technol. 52 (17), 9634–9645. https://doi.org/10.1021/acs.est.8b01948.

Boehm, A.B., Keymer, D.P., Shellenbarger, G.G., 2005. An analytical model of enterococci inactivation, grazing, and transport in the surf zone of a marine beach. Water Res. 39 (15), 3565–3578. https://doi.org/10.1016/j.watres.2005.06.026.

Bordalo, A.A., Onrassami, R., Dechsakulwatana, C., 2002. Survival of faecal indicator bacteria in tropical estuarine waters (Bangpakong River, Thailand). J. Appl. Microbiol. 93 (5), 864–871. https://doi.org/10.1046/j.1365-2672.2002.01760.x.

Bougeard, M., Le Saux, J.-C., Pérenne, N., Baffaut, C., Robin, M., Pommepuy, M., 2011. Modeling of Escherichia coli fluxes on a catchment and the impact on coastal water and shellfish Quality 1. JAWRA J. Am. Water Resour. Assoc. 47 (2), 350–366. https://doi.org/10.1111/j.1752-1688.2010.00520.x.

de Brauwere, A., Gourgue, O., de Brye, B., Servais, P., Ouattara, N.K., Deleersnijder, E., 2014. 'Integrated modelling of faecal contamination in a densely populated river–sea continuum (Scheldt River and Estuary)'. Sci. Total Environ. 468–469, 31–45. https://doi.org/10.1016/j.scitotenv.2013.08.019.

Brooks, L.E., Field, K.G., 2016. Bayesian meta-analysis to synthesize decay rate constant estimates for common fecal indicator bacteria. Water Res. 104, 262–271. https://doi.org/10.1016/j.watres.2016.08.005.

Bucci, V., Hoover, S., Hellweger, F.L., 2012. 'Modeling adaptive mutation of enteric bacteria in surface water using agent-based methods'. Water, Air, Soil Pollut. 223 (5), 2035–2049. https://doi.org/10.1007/s11270-011-1003-6.

Byappanahalli, M.N., Shively, D.A., Nevers, M.B., Sadowsky, M.J., Whitman, R.L., 2003. Growth and survival of Escherichia coli and enterococci populations in the macro-alga Cladophora (Chlorophyta). FEMS (Fed. Eur. Microbiol. Soc.) Microbiol. Ecol. 46 (2), 203–211. https://doi.org/10.1016/S0168-6496(03)00214-9.

Byappanahalli, M.N., Whitman, R.L., 2009. Clostridium botulinum type E occurs and grows in the alga Cladophora glomerata. Can. J. Fish. Aquat. Sci. 66 (6), 879–882. https://doi.org/10.1139/F09-052.

Cabelli, V.J., Dufour, A.P., McCABE, L.J., Levin, M.A., 1982. Swimming-associated gastroenteritis and water quality. Am. J. Epidemiol. 115 (4), 606–616. https://doi.org/10.1093/oxfordjournals.aje.a113342.

Carter, V., Rybicki, N.B., 1990. Light attenuation and submersed macrophyte distribution in the tidal Potomac River and estuary. Estuaries 13 (4), 441. https://doi.org/10.2307/1351788.

Champ, M.A., Gould, G.A., Bozzo, W.E., Ackleson, S.G., Vierra, K.C., 1980. Characterization of light extinction and attenuation in Chesapeake Bay, August, 1977. In: Estuarine Perspectives. Elsevier, pp. 263–277. https://doi.org/10.1016/B978-0-12-404060-1.50030-7.

Chancelier, J. Ph, Chebbo, G., Lucas-Aiguier, E., 1998. Estimation of settling velocities. Water Res. 32 (11), 3461–3471. https://doi.org/10.1016/S0043-1354(98)00114-6.

Chen, W.-B., Liu, W.-C., 2017. Investigating the fate and transport of fecal coliform contamination in a tidal estuarine system using a three-dimensional model. Mar. Pollut. Bull. 116 (1–2), 365–384. https://doi.org/10.1016/j.marpolbul.2017.01.031.

Cho, K.H., Cha, S.M., Kang, J.H., Lee, S.W., Park, Y., Kim, J.W., Kim, J.H., 2010. Meteorological effects on the levels of fecal indicator bacteria in an urban stream: a modeling approach. Water Res. Elsevier Ltd 44 (7), 2189–2202. https://doi.org/10.1016/j.watres.2009.12.051.

Cho, K.H., Pachepsky, Y.A., Oliver, D.M., Muirhead, R.W., Park, Y., Quilliam, R.S., Shelton, D.R., 2016. Modeling fate and transport of fecally-derived microorganisms at the watershed scale. State of the science and future opportunities', Wat. Res. 100, 38–56. https://doi.org/10.1016/j.watres.2016.04.064.

Chudoba, E.A., Mallin, M.A., Cahoon, L.B., Skrabal, S.A., 2013. Stimulation of fecal bacteria in ambient waters by experimental inputs of organic and inorganic phosphorus. Water Res. 47 (10), 3455–3466. https://doi.org/10.1016/j.watres.2013.03.047.

Cizek, A.R., Characklis, G.W., Krometis, L.-A., Hayes, J.A., Simmons, O.D., Di Lonardo, S., Alderisio, K.A., Sobsey, M.D., 2008. Comparing the partitioning

behavior of Giardia and Cryptosporidium with that of indicator organisms in stormwater runoff. Water Res. 42 (17), 4421–4438. https://doi.org/10.1016/j.watres.2008.06.020.
Coffey, R., Cummins, E., O' Flaherty, V., Cormican, M., 2010. Pathogen sources estimation and scenario analysis using the soil and water assessment tool (SWAT)', human and ecological risk assessment. Int. J. 16 (4), 913–933. https://doi.org/10.1080/10807039.2010.502051.
Cole, J.J., Caraco, N.F., Peierls, B.L., 1992. Can phytoplankton maintain positive carbon balance in a turbid, freshwater, tidal estuary? Limnol. Oceanogr. 37 (8), 1608–1617. https://doi.org/10.4319/lo.1992.37.8.1608.
Colford, J.M., Schiff, K.C., Griffith, J.F., Yau, V., Arnold, B.F., Wright, C.C., Gruber, J.S., Wade, T.J., Burns, S., Hayes, J., McGee, C., Gold, M., Cao, Y., Noble, R.T., Haugland, R., Weisberg, S.B., 2012. Using rapid indicators for Enterococcus to assess the risk of illness after exposure to urban runoff contaminated marine water. Water Res. 46 (7), 2176–2186. https://doi.org/10.1016/j.watres.2012.01.033.
Craig, D.L., Fallowfield, H.J., Cromar, N.J., 2002. Comparison of decay rates of faecal indicator organisms in recreational coastal water and sediment. Water Sci. Technol. Water Supply 2 (3), 131–138. https://doi.org/10.2166/ws.2002.0095.
Craig, D.L., Fallowfield, H.J., Cromar, N.J., 2004. Use of microcosms to determine persistence of Escherichia coli in recreational coastal water and sediment and validation with in situ measurements. J. Appl. Microbiol. 96 (5), 922–930. https://doi.org/10.1111/j.1365-2672.2004.02243.x.
Crump, B.C., Armbrust, E.V., Baross, J.A., 1999. Phylogenetic analysis of particle-attached and free-living bacterial communities in the Columbia River, its estuary, and the adjacent coastal ocean. Appl. Environ. Microbiol. 65 (7), 3192–3204. https://doi.org/10.1128/AEM.65.7.3192-3204.1999.
Davies, C.M., Bavor, H.J., 2000. The fate of stormwater-associated bacteria in constructed wetland and water pollution control pond systems. J. Appl. Microbiol. 89 (2), 349–360. https://doi.org/10.1046/j.1365-2672.2000.01118.x.
Davies-Colley, R.J., Bell, R.G., Donnison, A.M., 1994. Sunlight inactivation of enterococci and fecal coliforms in sewage effluent diluted in seawater. Appl. Environ. Microbiol. 60 (6), 2049–2058. https://doi.org/10.1128/AEM.60.6.2049-2058.1994.
Ducklow, H.W., Kirchman, David L., Rowe, Gilbert T., 1982. Production and vertical flux of attached bacteria in the Hudson River plume of the New York Bight as studied with floating sediment traps. Appl. Environ. Microbiol. 43, 8.
Evison, L.M., 1988. Comparative studies on the survival of indicator organisms and pathogens in fresh and sea water. Water Sci. Technol. 20 (11–12), 309–315. https://doi.org/10.2166/wst.1988.0300.
Feng, Z., Reniers, A., Haus, B.K., Solo-Gabriele, H.M., Kelly, E.A., 2016. Wave energy level and geographic setting correlate with Florida beach water quality. Mar. Pollut. Bull. 104 (1–2), 54–60. https://doi.org/10.1016/j.marpolbul.2016.02.011.
Findlay, S.E., 2005. Increased carbon transport in the Hudson River: unexpected consequence of nitrogen deposition? Front. Ecol. Environ. 3 (3), 133–137. https://doi.org/10.1890/1540-9295(2005)003[0133:ICTITH]2.0.CO;2.
Fong, T.-T., Lipp, E.K., 2005. Enteric viruses of humans and animals in aquatic environments: health risks, detection, and potential water quality assessment tools. Microbiol. Mol. Biol. Rev. 69 (2), 357–371. https://doi.org/10.1128/MMBR.69.2.357-371.2005.
Fries, J.S., Characklis, G.W., Noble, R.T., 2006. Attachment of fecal indicator bacteria to particles in the Neuse River Estuary, N.C. J. Environ. Eng. 132 (10), 1338–1345. https://doi.org/10.1061/(ASCE)0733-9372(2006)132:10(1338).
Fries, J.S., Characklis, G.W., Noble, R.T., 2008. Sediment-water exchange of Vibrio sp. and fecal indicator bacteria: implications for persistence and transport in the Neuse River Estuary, North Carolina, USA. Water Res. 42 (4–5), 941–950. https://doi.org/10.1016/j.watres.2007.09.006.
Fuchs, H.L., Neubert, M.G., Mullineaux, L.S., 2007. Effects of turbulence-mediated larval behavior on larval supply and settlement in tidal currents. Limnol. Oceanogr. 52 (3), 1156–1165. https://doi.org/10.4319/lo.2007.52.3.1156.
Fujioka, R.S., Hashimoto, H.H., Siwak, E.B., Young, R.H., 1981. Effect of sunlight on survival of indicator bacteria in seawater. Appl. Environ. Microbiol. 41 (3), 690–696.
Fujioka, R.S., Yoneyama, B.S., 2002. Sunlight inactivation of human enteric viruses and fecal bacteria. Water Sci. Technol. 46 (11–12), 291–295. https://doi.org/10.2166/wst.2002.0752.
Gao, G., Falconer, R.A., Lin, B., 2015. Modelling the fate and transport of faecal bacteria in estuarine and coastal waters. Mar. Pollut. Bull. 100 (1), 162–168. https://doi.org/10.1016/j.marpolbul.2015.09.011.
Garcia-Armisen, T., Servais, P., 2009. Partitioning and fate of particle-associated E. coli in river waters. Water Environ. Res. 81 (1), 21–28. https://doi.org/10.2175/106143008X304613.
Geyer, W.R., Signell, R.P., 1992. A reassessment of the role of tidal dispersion in estuaries and bays. Estuaries 15 (2), 97. https://doi.org/10.2307/1352684.
Gordon, D.M., Bauer, S., Johnson, J.R., 2002. The genetic structure of Escherichia coli populations in primary and secondary habitats. Microbiology (Read.) 148 (5), 1513–1522. https://doi.org/10.1099/00221287-148-5-1513.
Gutiérrez-Cacciabue, D., Cid, A.G., Rajal, V.B., 2016. How long can culturable bacteria and total DNA persist in environmental waters? The role of sunlight and solid particles. Sci. Total Environ. 539, 494–502. https://doi.org/10.1016/j.scitotenv.2015.07.138.
Hellweger, F.L., Masopust, P., 2008. Investigating the fate and transport of Escherichia coli in the Charles River, Boston, using high-resolution observation and modeling. JAWRA J. Am. Water Resour. Assoc. 44 (2), 509–522. https://doi.org/10.1111/j.1752-1688.2008.00179.x.
Hess-Erga, O., Kihle Attramadal, K., Vadstein, O., 2008. Biotic and abiotic particles protect marine heterotrophic bacteria during UV and ozone disinfection. Aquat. Biol. 4, 147–154. https://doi.org/10.3354/ab00105.
Hipsey, M.R., Antenucci, J.P., Brookes, J.D., 2008. A generic, process-based model of microbial pollution in aquatic systems: microbial pollution IN aquatic systems. Water Resour. Res. 44 (7) https://doi.org/10.1029/2007WR006395.
Horman, A., Rimhanen-Finne, R., Maunula, L., von Bonsdorff, C.-H., Torvela, N., Heikinheimo, A., Hanninen, M.-L., 2004. Campylobacter spp., Giardia spp., Cryptosporidium spp., noroviruses, and indicator organisms in surface water in southwestern Finland, 2000-2001. Appl. Environ. Microbiol. 70 (1), 87–95. https://doi.org/10.1128/AEM.70.1.87-95.2004.
Howell, J.M., Coyne, M.S., Cornelius, P.L., 1996. Effect of sediment particle size and temperature on fecal bacteria mortality rates and the fecal coliform/fecal streptococci ratio. J. Environ. Qual. 25, 1216–1220. https://doi.org/10.2134/jeq1996.00472425002500060007x.
IDEXX Laboratories, 2013. Insert and Most Probable Number (MPN) Table. IDEXX Laboratories, Westbrook, ME.
Imamura, G.J., Thompson, R.S., Boehm, A.B., Jay, J.A., 2011. Wrack promotes the persistence of fecal indicator bacteria in marine sands and seawater: beach wrack: FIB reservoir. FEMS (Fed. Eur. Microbiol. Soc.) Microbiol. Ecol. 77 (1), 40–49. https://doi.org/10.1111/j.1574-6941.2011.01082.x.
Jamieson, R.C., Joy, D.M., Lee, H., Kostaschuk, R., Gordon, R.J., 2005a. Resuspension of sediment-associated Escherichia coli in a natural stream. J. Environ. Qual. 34 (2), 581–589. https://doi.org/10.2134/jeq2005.0581.
Jamieson, R., Gordon, R., Joy, D., Lee, H., 2004. Assessing microbial pollution of rural surface waters. Agric. Water Manag. 70 (1), 1–17. https://doi.org/10.1016/j.agwat.2004.05.006.
Jamieson, R., Joy, D., Lee, H., Kostaschuk, R., Gordon, R., 2005b. Transport and deposition of sediment-associated *Escherichia coli* in natural streams. Water Res. 39 (12), 2665–2675. https://doi.org/10.1016/j.watres.2005.04.040.
Jeng, H.C., Sinclair, R., Daniels, R., Englande, A.J., 2005. Survival of Enterococci facalis in estuarine sediments. Int. J. Environ. Stud. 62 (3), 283–291. https://doi.org/10.1080/0020723042000275132.
Jones, S.E., Jago, C.F., 1996. Determination of settling velocity in the Elbe estuary using quisset tubes. J. Sea Res. 36 (1–2), 63–67. https://doi.org/10.1016/S1385-1101(96)90772-8.
Kay, D., Stapleton, C.M., Wyer, M.D., McDonald, A.T., Crowther, J., Paul, N., Jones, K., Francis, C., Watkins, J., Wilkinson, J., Humphrey, N., Lin, B., Yang, L., Falconer, R.A., Gardner, S., 2005. Decay of intestinal enterococci concentrations in high-energy estuarine and coastal waters: towards real-time T90 values for modelling faecal indicators in recreational waters. Water Res. 39 (4), 655–667. https://doi.org/10.1016/j.watres.2004.11.014.
Kim, J.-W., Pachepsky, Y.A., Shelton, D.R., Coppock, C., 2010. Effect of streambed bacteria release on E. coli concentrations: monitoring and modeling with the modified SWAT. Ecol. Model. 221 (12), 1592–1604. https://doi.org/10.1016/j.ecolmodel.2010.03.005.
Kiørboe, T., Jackson, G.A., 2001. Marine snow, organic solute plumes, and optimal chemosensory behavior of bacteria. Limnol. Oceanogr. 46 (6), 1309–1318. https://doi.org/10.4319/lo.2001.46.6.1309.
Krometis, L.A.H., Characklis, G.W., Simmons, O.D., Dilts, M.J., Likirdopulos, C.A., Sobsey, M.D., 2007. Intra-storm variability in microbial partitioning and microbial loading rates. Water Res. 41 (2), 506–516. https://doi.org/10.1016/j.watres.2006.09.029.
Lee, C.W., Ng, A.Y.F., Bong, C.W., Narayanan, K., Sim, E.U.H., Ng, C.C., 2011. Investigating the decay rates of Escherichia coli relative to Vibrio parahemolyticus and Salmonella Typhi in tropical coastal waters. Water Res. 45 (4), 1561–1570. https://doi.org/10.1016/j.watres.2010.11.025.
Litsky, W., Mallmann, W.L., Fifield, C.W., 1953. A new medium for the detection of enterococci in water. Am. J. Public Health Nation's Health 43 (7), 873–879. https://doi.org/10.2105/AJPH.43.7.873.
Lleo, M., Del, M., Bonato, B., Benedetti, D., Canepari, P., 2005. Survival of enterococcal species in aquatic environments. FEMS (Fed. Eur. Microbiol. Soc.) Microbiol. Ecol. 54 (2), 189–196. https://doi.org/10.1016/j.femsec.2005.03.016.
Lund-Hansen, L.C., 2004. 'Diffuse attenuation coefficients Kd(PAR) at the estuarine North Sea–Baltic Sea transition: time-series, partitioning, absorption, and scattering. Estuar. Coast Shelf Sci. 61 (2), 251–259. https://doi.org/10.1016/j.ecss.2004.05.004.
Lyons, M.M., Lau, Y.-T., Carden, W.E., Ward, J.E., Roberts, S.B., Smolowitz, R., Vallino, J., Allam, B., 2007. Characteristics of marine aggregates in shallow-water ecosystems: implications for disease ecology. EcoHealth 4 (4), 406–420. https://doi.org/10.1007/s10393-007-0134-0.
Lyons, M., Ward, J., Gaff, H., Hicks, R., Drake, J., Dobbs, F., 2010. Theory of island biogeography on a microscopic scale: organic aggregates as islands for aquatic pathogens. Aquat. Microb. Ecol. 60 (1), 1–13. https://doi.org/10.3354/ame01417.
Madge, B.A., Jensen, J.N., 2006. Ultraviolet disinfection of fecal coliform in municipal wastewater: effects of particle size. Water Environ. Res. 78 (3), 294–304. https://doi.org/10.2175/106143005X94385.

Maïga, Y., Denyigba, K., Wethe, J., Ouattara, A.S., 2009. Sunlight inactivation of Escherichia coli in waste stabilization microcosms in a sahelian region (Ouagadougou, Burkina Faso). J. Photochem. Photobiol. B Biol. 94 (2), 113–119. https://doi.org/10.1016/j.jphotobiol.2008.10.008.

Malarkey, J., Jago, C.F., Hübner, R., Jones, S.E., 2013. A simple method to determine the settling velocity distribution from settling velocity tubes. Continent. Shelf Res. 56, 82–89. https://doi.org/10.1016/j.csr.2013.01.018.

Malloy, K.D., Holman, M.A., Mitchell, D., Detrich, H.W., 1997. Solar UVB-induced DNA damage and photoenzymatic DNA repair in antarctic zooplankton. Proc. Natl. Acad. Sci. Unit. States Am. 94 (4), 1258–1263. https://doi.org/10.1073/pnas.94.4.1258.

Maraccini, P.A., Ferguson, D.M., Boehm, A.B., 2012. Diurnal variation in Enterococcus species composition in polluted ocean water and a potential role for the enterococcal carotenoid in protection against photoinactivation. Appl. Environ. Microbiol. 78 (2), 305–310. https://doi.org/10.1128/AEM.06821-11.

Maraccini, P.A., Mattioli, M.C.M., Sassoubre, L.M., Cao, Y., Gri, J.F., Ervin, J.S., Werfhorst, L.C.V.D., Boehm, A.B., 2016. Solar Inactivation of Enterococci and Escherichia coli in Natural Waters: Effects of Water Absorbance and Depth. https://doi.org/10.1021/acs.est.6b00505.

Mattioli, M.C., Sassoubre, L.M., Russell, T.L., Boehm, A.B., 2017. Decay of sewage-sourced microbial source tracking markers and fecal indicator bacteria in marine waters. Wat. Res. 108, 106–114. https://doi.org/10.1016/j.watres.2016.10.066.

McCambridge, J., McMeekin, T.A., 1981. Effect of solar radiation and predacious microorganisms on survival of fecal and other bacteria. Appl. Environ. Microbiol. 41 (5), 1083–1087. https://doi.org/10.1128/AEM.41.5.1083-1087.1981.

Menon, P., Billen, G., Servais, P., 2003. Mortality rates of autochthonous and fecal bacteria in natural aquatic ecosystems. Water Res. 37 (17), 4151–4158. https://doi.org/10.1016/S0043-1354(03)00349-X.

Morel, A., Gentili, B., Claustre, H., Babin, M., Bricaud, A., Ras, J., Tièche, F., 2007. 'Optical properties of the "clearest" natural waters'. Limnol. Oceanogr. 52 (1), 217–229. https://doi.org/10.4319/lo.2007.52.1.0217.

Mote, B.L., Turner, J.W., Lipp, E.K., 2012. Persistence and growth of the fecal indicator bacteria enterococci in detritus and natural estuarine plankton communities. Appl. Environ. Microbiol. 78 (8), 2569–2577. https://doi.org/10.1128/AEM.06902-11.

Neitsch, S.L., Arnold, J.G., Kiniry, J.R., Williams, J.R., 2009. Soil and Water Assessment Tool Theoretical Documentation, p. 494. https://archive.epa.gov/scipoly/sap/meetings/web/pdf/swat_theory.pdf.

Nevers, M.B., Boehm, A.B., 2011. Modeling fate and transport of fecal bacteria in surface water. In: Sadowsky and Whitman (Eds) the Fecal Bacteria. American Society of Microbiology, pp. 165–188. https://doi.org/10.1128/9781555816865.ch8.

Niazi, M., Obropta, C., Miskewitz, R., 2015. Pathogen transport and fate modeling in the Upper Salem River Watershed using SWAT model. J. Environ. Manag. 151, 167–177. https://doi.org/10.1016/j.jenvman.2014.12.042.

Noble, R.T., Lee, I.M., Schiff, K.C., 2004. Inactivation of indicator micro-organisms from various sources of faecal contamination in seawater and freshwater. J. Appl. Microbiol. 96 (3), 464–472. https://doi.org/10.1111/j.1365-2672.2004.02155.x.

Okabe, S., Shimazu, Y., 2007. 'Persistence of host-specific Bacteroides–Prevotella 16S rRNA genetic markers in environmental waters: effects of temperature and salinity'. Appl. Microbiol. Biotechnol. 76 (4), 935–944. https://doi.org/10.1007/s00253-007-1048-z.

O'Mullan, G.D., Dueker, E.M., Juhl, A.R., 2017. Challenges to managing microbial fecal pollution in coastal environments: extra-enteric ecology and microbial exchange among water, sediment, and air', current pollution reports. Curr. Pollut. Rep. 3 (1), 1–16. https://doi.org/10.1007/s40726-016-0047-z.

O'Mullan, G.D., Juhl, A.R., Reichert, R., Schneider, E., Martinez, N., 2019. Patterns of sediment-associated fecal indicator bacteria in an urban estuary: benthic-pelagic coupling and implications for shoreline water quality. Sci. Total Environ. 656, 1168–1177. https://doi.org/10.1016/j.scitotenv.2018.11.405.

Orton, P.M., Kineke, G.C., 2001. 'Comparing calculated and observed vertical suspended-sediment distributions from a Hudson River estuary turbidity maximum. Estuar. Coast Shelf Sci. 52, 401–410. https://doi.org/10.1006/ecss.2000.0747, 10.1006.

Owen, M.W., 1976. Determination of the settling velocities of cohesive muds. Report No. IT 161, 8.

Palmateer, G.A., McLean, D.E., Walsh, M.J., Kutas, W.L., Janzen, E.M., Hocking, D.E., 1989. A study of contamination of suspended stream sediments with Escherichia coli. Toxic. Assess. 4 (3), 377–397. https://doi.org/10.1002/tox.2540040313.

Pandey, P.K., Soupir, M.L., Ikenberry, C.D., Rehmann, C.R., 2016. Predicting streambed sediment and water column Escherichia coli levels at watershed scale. JAWRA J. Am. Water Resour. Assoc. 52 (1), 184–197. https://doi.org/10.1111/1752-1688.12373.

Qualls, R., Flynn, M., Johnson, J.D., 1983. The role of suspended particles in ultraviolet disinfection. J. Water Pollut. Control Fed. 55 (10), 1280–1185.

Quay, P.D., Broecker, W.S., Hesslein, R.H., Schindler, D.W., 1980. Vertical diffusion rates determined by tritium tracer experiments in the thermocline and hypolimnion of two lakes 1,2: vertical diffusion rates in lakes. Limnol. Oceanogr. 25 (2), 201–218. https://doi.org/10.4319/lo.1980.25.2.0201.

Rippy, M.A., Franks, P.J.S., Feddersen, F., Guza, R.T., Moore, D.F., 2013a. Factors controlling variability in nearshore fecal pollution: the effects of mortality. Mar. Pollut. Bull. 66 (1–2), 191–198. https://doi.org/10.1016/j.marpolbul.2012.09.003.

Rippy, M.A., Franks, P.J.S., Feddersen, F., Guza, R.T., Moore, D.F., 2013b. Physical dynamics controlling variability in nearshore fecal pollution: fecal indicator bacteria as passive particles. Mar. Pollut. Bull. 66 (1–2), 151–157. https://doi.org/10.1016/j.marpolbul.2012.09.030.

Rose, K.C., Williamson, C.E., Schladow, S.G., Winder, M., Oris, J.T., 2009. Patterns of spatial and temporal variability of UV transparency in Lake Tahoe, California-Nevada: UV transparency OF Lake Tahoe, CA-NV. J. Geophys. Res.: Biogeosci. 114 (G2) https://doi.org/10.1029/2008JG000816 n/a-n/a.

Russo, S.A., Hunn, J., Characklis, G.W., 2011. Considering bacteria-sediment associations in microbial fate and transport modeling. J. Environ. Eng. 137 (8), 697–706. https://doi.org/10.1061/(ASCE)EE.1943-7870.0000363.

Sadeghi, A.M., Arnold, J.G., 2002. A SWAT/microbial sub-model for predicting pathogen loadings in surface and groundwater at watershed and basin scales. In: Total Maximum Daily Load (TMDL): Environmental Regulations, Proceedings of 2002 Conference. American Society of Agricultural and Biological Engineers. https://doi.org/10.13031/2013.7529.

Sanders, B.F., Arega, F., Sutula, M., 2005. Modeling the dry-weather tidal cycling of fecal indicator bacteria in surface waters of an intertidal wetland. Water Res. 39 (14), 3394–3408. https://doi.org/10.1016/j.watres.2005.06.004.

Schuch, A.P., Menck, C.F.M., 2010. The genotoxic effects of DNA lesions induced by artificial UV-radiation and sunlight. J. Photochem. Photobiol. B Biol. 99 (3), 111–116. https://doi.org/10.1016/j.jphotobiol.2010.03.004.

Schulz, C.J., Childers, G.W., 2011. Fecal Bacteroidales diversity and decay in response to variations in temperature and salinity. Appl. Environ. Microbiol. 77 (8), 2563–2572. https://doi.org/10.1128/AEM.01473-10.

Shanks, A., Reeder, M., 1993. Reducing microzones and sulfide production in marine snow. Mar. Ecol. Prog. Ser. 96, 43–47. https://doi.org/10.3354/meps096043.

Sinton, L.W., Davies-Colley, R.J., Bell, R.G., 1994. Inactivation of enterococci and fecal coliforms from sewage and meatworks effluents in seawater chambers. Appl. Environ. Microbiol 60 (6), 2040–2048. https://doi.org/10.1128/AEM.60.6.2040-2048.

Sinton, L.W., Hall, C.H., Lynch, P.A., Davies-Colley, R.J., 2002. Sunlight inactivation of fecal indicator bacteria and bacteriophages from waste stabilization pond effluent in fresh and saline waters. Appl. Environ. Microbiol. 68 (3), 1122–1131. https://doi.org/10.1128/AEM.68.3.1122-1131.2002.

Stacey, M.T., Monismith, S.G., Burau, J.R., 1999. Observations of turbulence in a partially stratified estuary. J. Phys. Oceanogr. 29, 21. https://doi.org/10.1175/1520-0485(1999)029<1950:OOTIAP>2.0.CO;2.

Steets, B.M., Holden, P.A., 2003. A mechanistic model of runoff-associated fecal coliform fate and transport through a coastal lagoon. Water Res. 37 (3), 589–608. https://doi.org/10.1016/S0043-1354(02)00312-3.

Stross, R.G., Sokol, R.C., 1989. Runoff and flocculation modify underwater light environment of the Hudson River estuary. Estuar. Coast Shelf Sci. 29 (4), 305–316. https://doi.org/10.1016/0272-7714(89)90030-9.

Surbeck, C.Q., Jiang, S.C., Grant, S.B., 2010. Ecological control of fecal indicator bacteria in an urban stream. Environ. Sci. Technol. 44 (2), 631–637. https://doi.org/10.1021/es903496m.

Suter, E., Juhl, A.R., O'Mullan, G.D., 2011. Particle association of Enterococcus and total bacteria in the lower Hudson River estuary, USA. J. Water Resour. Protect. (10), 715–725. https://doi.org/10.4236/jwarp.2011.310082, 03.

Swift, T.J., Perez-Losada, J., Schladow, S.G., Reuter, J.E., Jassby, A.D., Goldman, C.R., 2006. Water clarity modeling in Lake Tahoe: linking suspended matter characteristics to Secchi depth. Aquat. Sci. 68 (1), 1–15. https://doi.org/10.1007/s00027-005-0798-x.

Toole, J.M., Schmitt, R.W., Polzin, K.L., 1994. Estimates of diapycnal mixing in the abyssal ocean. Science 264 (5162), 1120–1123. https://doi.org/10.1126/science.264.5162.1120.

Tyler, J.E., 1973. Data Report of the Discoverer Expedition. SIO Ref 73-16. University California. Scripps Institution of Oceanography, Visibility Laboratory, San Diego.

US EPA, 2002. Method 1600: Enterococci in Water by Membrane Filtration Using Membrane-Enterococcus Indoxyl-B-D-Glucoside Agar (mEI). EPA 821-R-02-022. Office of Water.

US EPA, 2012. Recreational Water Quality Criteria. OFFICE of WATER 820-F-12–058.

Vermeulen, L.C., de Kraker, J., Hofstra, N., Kroeze, C., Medema, G., 2015. 'Modelling the impact of sanitation, population growth and urbanization on human emissions of Cryptosporidium to surface waters—a case study for Bangladesh and India'. Environ. Res. Lett. 10 (9) https://doi.org/10.1088/1748-9326/10/9/094017, 094017.

Wade, T.J., Pai, N., Eisenberg, J.N.S., Colford, J.M., 2003. Do U.S. Environmental Protection Agency water quality guidelines for recreational waters prevent gastrointestinal illness? A systematic review and meta-analysis. EHP (Environ. Health Perspect.) 111 (8), 1102–1109. https://doi.org/10.1289/ehp.6241.

Walters, E., Graml, M., Behle, C., Müller, E., Horn, H., 2014. Influence of particle association and suspended solids on UV inactivation of fecal indicator bacteria in an urban river. Water Air Soil Pollut. 225 (1) https://doi.org/10.1007/s11270-013-1822-8.

Wen, B., Georgas, N., Dujardins, C., Kumaraswamy, A., Cohn, A., 2017. Modeling pathogens for oceanic contact recreation advisories in the New York City area

using total event simulations. Ecol. Mod. 365, 93–105. https://doi.org/10.1016/j.ecolmodel.2017.09.021. Elsevier B.V.

Whitman, R.L., Nevers, M.B., Korinek, G.C., Byappanahalli, M.N., 2004. Solar and temporal effects on Escherichia coli concentration at a Lake Michigan swimming beach. Appl. Environ. Microbiol. 70 (7), 4276–4285. https://doi.org/10.1128/AEM.70.7.4276-4285.2004.

Wodka, M.C., Effler, S.W., Driscoll, C.T., Field, S.D., Devan, S.P., 1983. 'Diffusivity-Based flux of phosphorus in Onondaga Lake'. J. Environ. Eng. 109 (6), 1403–1415. https://doi.org/10.1061/(ASCE)0733-9372(1983)109:6(1403).

Wu, J., Rees, P., Storrer, S., Alderisio, K., Dorner, S., 2009. Fate and transport modeling of potential pathogens: the contribution from sediments. JAWRA J. Am. Water Resour. Assoc. 45 (1), 35–44. https://doi.org/10.1111/j.1752-1688.2008.00287.x.

Yamahara, K.M., Walters, S.P., Boehm, A.B., 2009. Growth of enterococci in unaltered, unseeded beach sands subjected to tidal wetting. Appl. Environ. Microbiol. 75 (6), 1517–1524. https://doi.org/10.1128/AEM.02278-08.

Yang, L., Lin, B., Falconer, R.A., 2008. Modelling enteric bacteria level in coastal and estuarine waters. Proc. Inst. Civil Eng. - Eng. Comput. Mechan. 161 (4), 179–186. https://doi.org/10.1680/eacm.2008.161.4.179.

Yeh, T.Y., Ke, T.Y., Lin, Y.L., 2011. Algal growth control within natural water purification systems: macrophyte light shading effects. Water, Air, Soil Pollut. 214 (1–4), 575–586. https://doi.org/10.1007/s11270-010-0447-4.

Appendix A

Table A.1 Environmental Data. Environmental data for temperature- and light-dependent growth rate experiments. Note the variability in starting concentration of enterococci and how it does not correlate to the variability in particle association ($r^2 = 0.15$). It is noted for each experiment which fraction was tested.

Treatment	Experiment	Date	Time	Site	Salinity	Temp (°C)	Secchi Disk (cm)	Tide	O2 (%)	O2 (mg/L)	Precip past 3 d (in)	Enterococci (CFU/ 100mL)	Particle Association (%)	Fraction
Temp	1	2/26/2018	11:02	Piermont Pier	0.85	3.7	38	low, outgoing	98.4	13	0.93	261	36	FL, PA
Temp	2	2/26/2018	10:30	Nyack	0.27	3.4	48	low, outgoing	100.1	13.3	0.93	63	20	FL, PA
Temp	3	3/26/2018	10:35	Piermont Pier	4.28	5.5	44	out, mid	95	11.9	0	85	70	FL, PA
Temp	4	4/3/2018	9:40	Piermont Pier	1.81	5.6	40	low, incoming	96.8	12.1	0.46	85	70	FL, PA
Temp	5	4/17/2018	8:40	Piermont Pier	3.75	7.8	25	low, incoming	95.4	11	2.76	341	26	FL, PA
Temp	6	4/17/2018	8:40	Piermont Pier	3.75	7.8	25	low, incoming	95.4	11	2.76	341	26	FL, PA
Light	1	5/8/2018	12:13	Sparkill	0.4	17.5			92.7	8.9	0.02	14	0	FL
Light	2	5/8/2018	12:13	Sparkill	0.4	17.5			92.7	8.9	0.02	14	0	FL
Light	3	5/29/2018	9:54	Sparkill	0.4	16.5					0.05	175	0	FL
Light	4	5/29/2018	9:54	Sparkill	0.4	16.5					0.05	175	0	FL
Light	5	7/30/2018	14:00	Piermont SPDES	6.35	25.6		high, outgoing			0.47	103	0	FL, PA
Light	6	7/30/2018	14:00	Piermont SPDES	6.35	25.6		high, outgoing			0.47	103	0	FL, PA
Light	7	8/6/2018	16:20	Piermont SPDES	4.33	35.5		high, incoming			0.64	804	45	FL
Light	8	8/6/2018	16:20	Piermont SPDES	4.33	35.5		high, incoming			0.64	804	45	FL
Light	9	5/31/2019	10:04	Piermont SPDES	1.95	19.8		high, outgoing	76.9	6.9	2.14	96	1	FL, PA
Light	10	5/31/2019	10:04	Piermont SPDES	1.95	19.8		high, outgoing	76.9	6.9	2.14	96	1	FL, PA
MEAN					2.60	16.48	36.67		95.81		0.73	240.52	24.14	

Table A.2 Temperature-Dependent Experiments Data. Raw data from each temperature-dependent growth experiment for all fractions. Growth rates are reported as (day^{-1}).

	FL			PA			Total		
n (#)	5 ℃	18 ℃	28 ℃	5 ℃	18 ℃	28 ℃	5 ℃	18 ℃	28 ℃
1	-0.02	-0.11	-0.07	-0.46	-0.49	-0.72	-0.17	-0.24	-0.26
2	0.20	-0.17	0.37	0.27	-0.13	0.00	0.23	-0.15	0.26
3	-0.40	-1.34	-0.40	-0.07	0.22	-0.27	-0.31	-0.46	-0.37
4	-0.07	0.18	-0.10	-0.14	0.28	-0.07	-0.09	0.21	-0.09
5	0.10	-0.38	-0.69	1.16	1.03	1.05	0.29	-0.03	-0.14
6	0.27	-0.35	-0.84	1.04	1.07	0.82	0.38	0.01	-0.34
MEAN	0.01	-0.36	-0.29	0.30	0.33	0.13	0.30	0.33	0.13
Std Dev	0.24	0.52	0.45	0.66	0.62	0.67	0.28	0.23	0.23

Table A.3 Light-Dependent Experiments Data. Raw data and light-normalized growth-rates with incident solar irradiance measured for the duration of each experiment.

n (#)	**Norm FL Rate** ($\boldsymbol{day^{-1}}$)	**Norm PA Rate** ($\boldsymbol{day^{-1}}$)	**Norm Total Rate** ($\boldsymbol{day^{-1}}$)	**Light** $\left(\frac{\mu mol\ photon}{m^2}\right)$	**Raw FL Rate** ($\boldsymbol{day^{-1}}$)	**Raw PA Rate** ($\boldsymbol{day^{-1}}$)	**Raw Total Rate** ($\boldsymbol{day^{-1}}$)
1	-18.48		-16.36	5.90	-23.35		-20.67
2	-25.07		-25.07	5.90	-31.67		-31.67
3	-75.25		-75.40	12.07	-46.47		-46.56
4	-51.09		-51.17	12.07	-31.55		-31.60
5	-15.95	-7.89	-11.79	3.11	-38.22	-18.92	-28.26
6	-14.49	-16.94	-15.22	3.11	-34.73	-40.61	-36.47
7	-24.44		-17.03	3.46	-52.58		-36.64
8	-22.66		-10.88	3.46	-48.76		-23.41
9	-39.14	-22.85	-36.27	12.73	-22.92	-13.38	-21.24
10	-46.58	-18.23	-40.08	12.73	-27.28	-10.68	-23.48
MEAN	-33.31	-16.48	-29.93	6.14			
Std Dev	19.50	6.26	20.94	3.84			

Table A.4 Initial conditions for settling experiments. Note that mass-based TSS was linearly related to turbidity measured optically in the original sample ($r^2 = 0.99$).

Date	Temperature(˚C)	Salinity	Turbidity (NTU)	Initial TSS (g/l)	% organic TSS	[Enterococci] (CFU/100 ml)	Particle Association (%)
9/19/2012	22.8	15.2	24	0.029	18.4	72	57
10/20/2012	18.2	10.4	26	0.027	14.1	252	59
10/25/2012	16.8	6	17	0.02	19.8	1298	72
4/6/2013	6.5	5.7	63	0.058	11.5	1013	50
4/7/2013	6.8	6.8	48	0.046	13.7	441	18

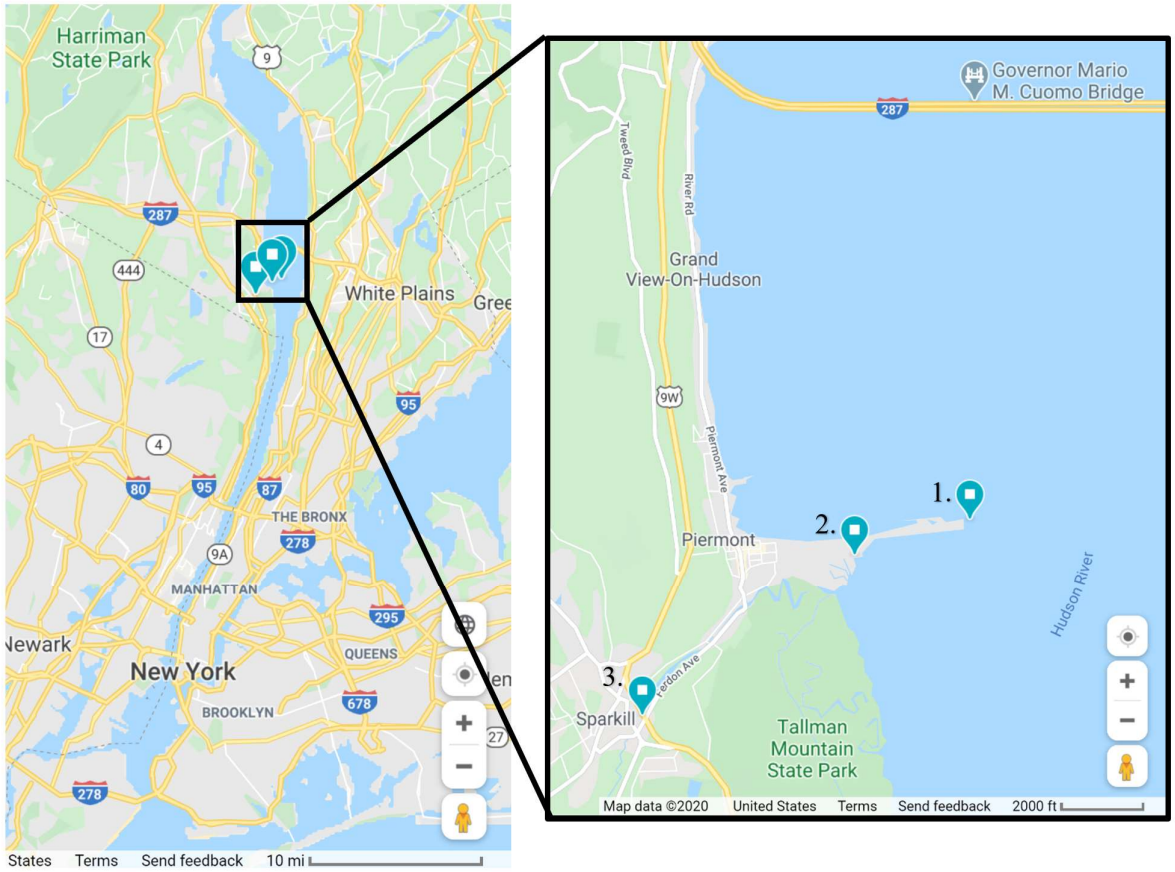

Fig. A.1 Map of Sample Sites

A map noting the location of the two Hudson River sampling sites on Piermont Pier in Piermont, NY and one site in Sparkill, NY. The field sites are:1) near the combined outfall of the Orangetown Wastewater Treatment Plant and the Rockland County Sewer District (41.043, -73.896), 2) near a sewage pump station that occasionally overflows (State Pollutant Discharge Elimination System, Permitted Discharge Point No. NY 002605; 41.041, -73.906), and 3) the commonly contaminated tributary, Sparkill Creek (41.031, -73.924). Map copyright GoogleMaps.

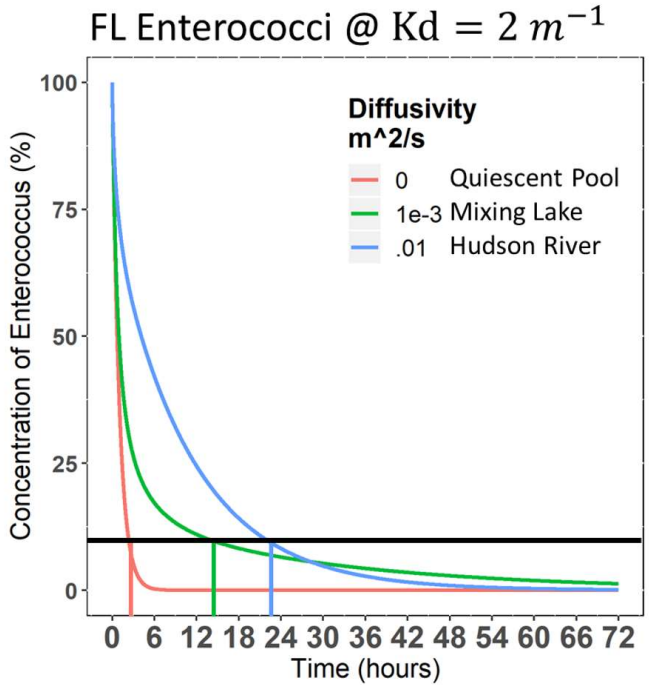

Fig. A.2 Example Measurement of Simulation T_{90}
Enterococci population decays according to model parameter values. The time when 90% of the population has decayed is then marked at T_{90}, denoted here by the horizontal black line. This example holds K_d constant at 2 meters^{-1} and varies diffusivity. Each pairing of K_d and D values will have a different T_{90} calculation, marked along the x-axis by the colored vertical lines.

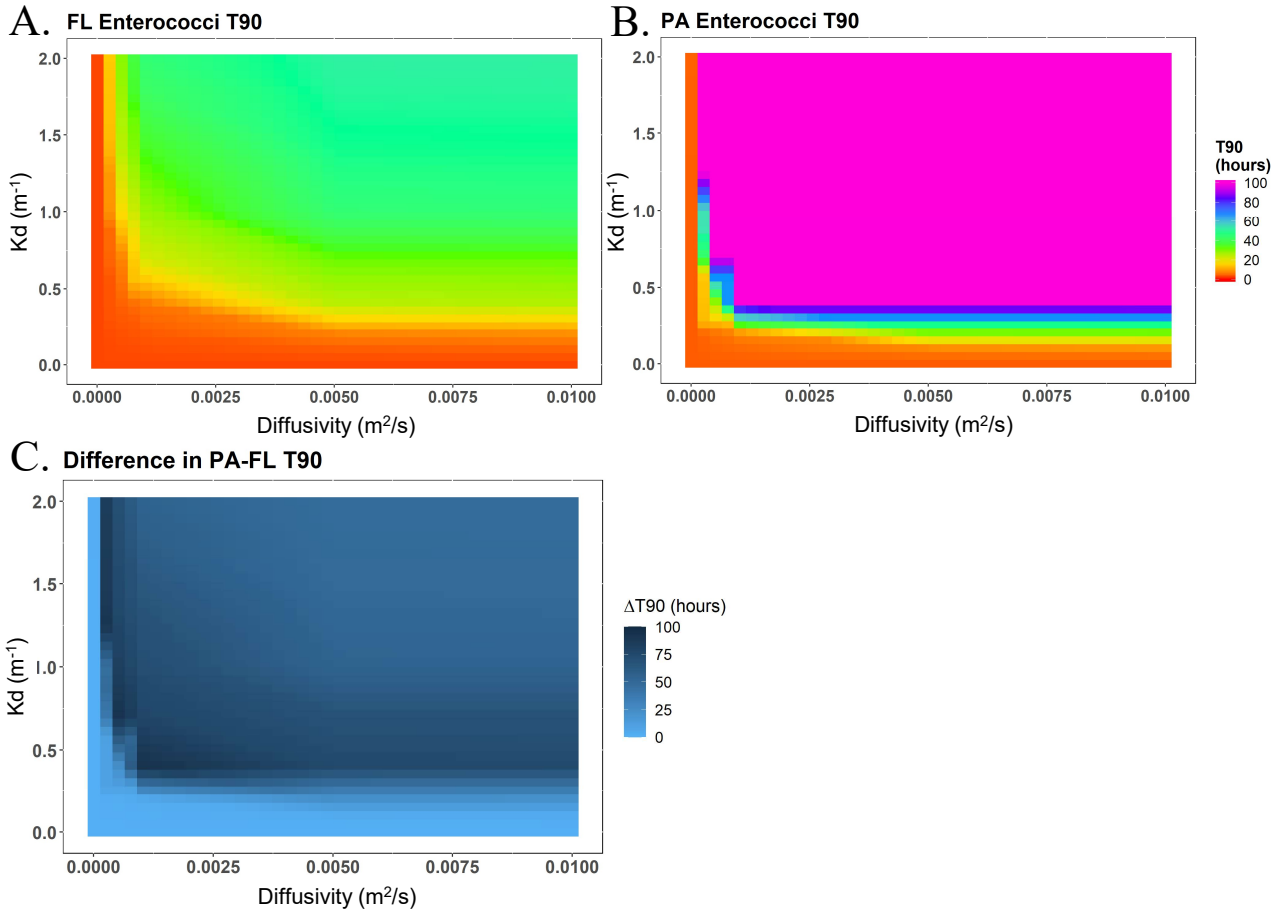

Fig. A.3. Diel Cycle T_{90} with 4 Hour Delay.

T_{90} for free-living (A) and particle-associated (B) enterococci is plotted along a wide range of physically-relevant K_d and D values. The difference in PAT_{90} and FLT_{90} (B-A) is consistently greater than 0 (C). Discharge occurred 4 hours following sunrise and the simulation was run using standard run values.

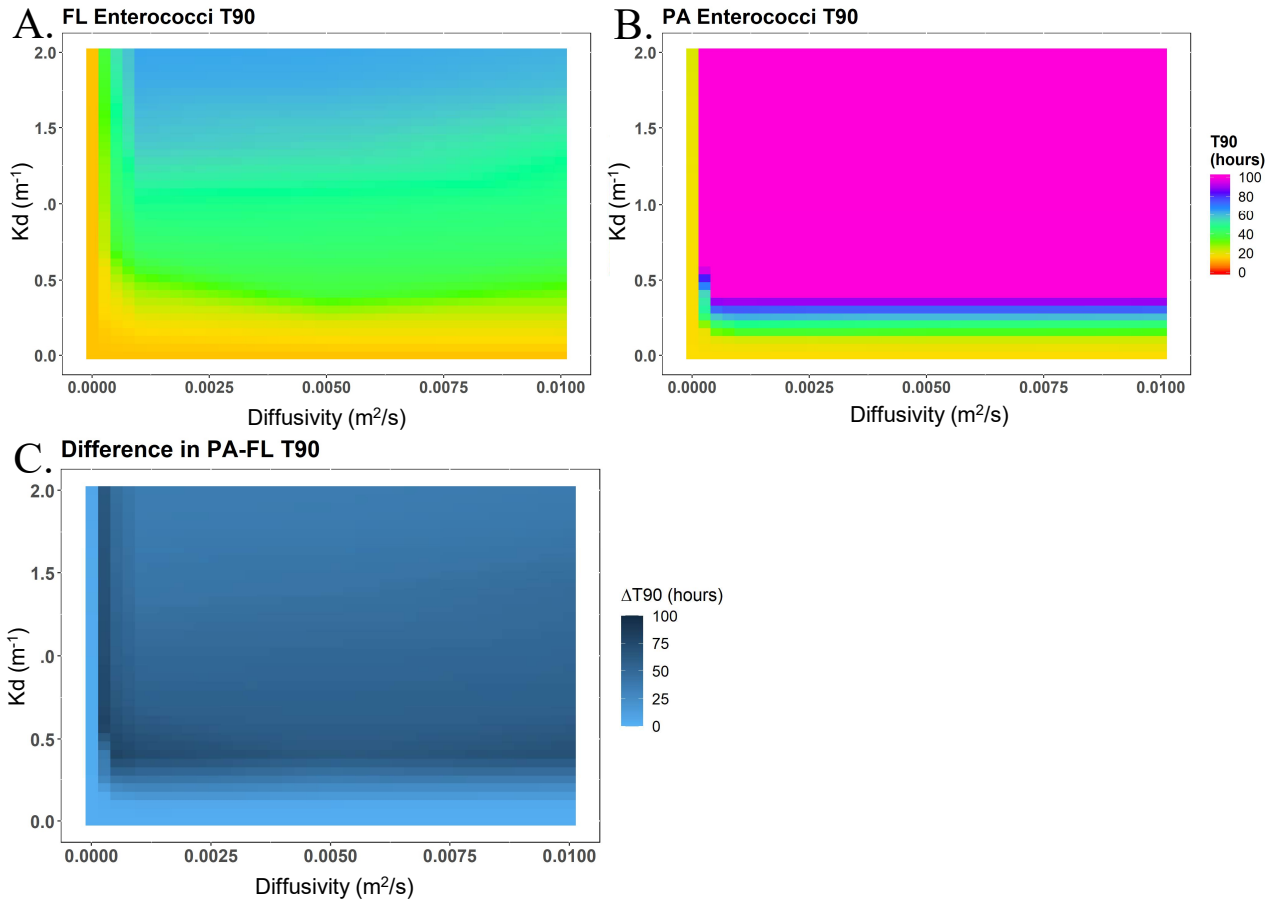

Fig. A.4. Diel Cycle T_{90} with 12 Hour Delay.
T_{90} for free-living (A) and particle-associated (B) enterococci is plotted along a wide range of physically-relevant K_d and D values. The difference in T_{90} between particle-associated and free-living enterococci (B-A) is always greater than 0 (C). Discharge occurred 12 hours following sunrise, so 4 hours prior to sunset in the 16-hour day/8-hour night cycle. The simulation was run using standard run values.

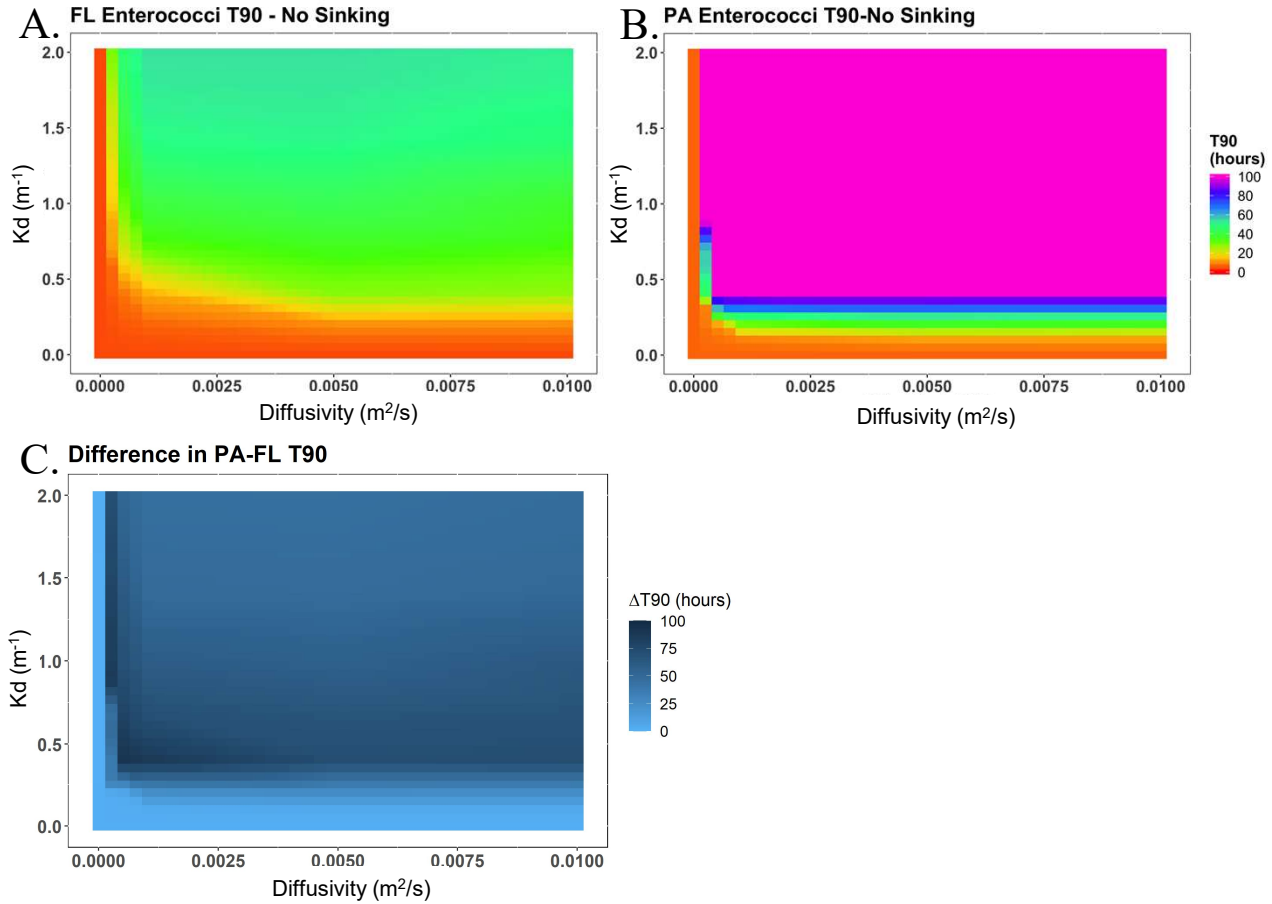

Fig. A.5. Standard Model T_{90} with Sinking Rate Removal

T_{90} for free-living (A) and particle-associated (B) enterococci is plotted along a wide range of physically-relevant K_d and D values. The difference in PAT_{90} and FLT_{90} (B-A) is consistently greater than 0 (C). For this model run, the sinking term was removed, altering PAT_{90}, but not FLT_{90} from Fig.2. Discharge occurred directly prior to sunrise in the 16-hour day/8-hour night cycle and the simulation was run with standard run values.